

D7.2

The assessment of flood risk under the current climate for three storylines

RECEIPT project information

Project full title	Remote Climate Effects and their Impact on European sustainability, Policy and Trade
Project acronym	RECEIPT
Grant agreement number	820712
Start date and duration	01/09/2019, 48 months
Website	www.climatestorylines.eu

Deliverable information

Work package number	Work Package 7
Work package title	Sea level rise, infrastructure and coastal flooding
Deliverable number	D7.2
Deliverable title	The assessment of flood risk under the current climate for three storylines
Description	Report
Lead beneficiary	VU-IVM
Author (s)	Elco Koks (VU-IVM), Sadhana Nirandjan (VU-IVM), Dewi Le Bars (KNMI), Arthur Hraat Essenfelder (CMCC), Paul Sayers (SPL)
Contributor (s)	
Revision number	V1.0
Revision date	2-9-2021

Dissemination level of the document

<input checked="" type="checkbox"/>	PU	Public
<input type="checkbox"/>	PP	Restricted to other programme participants
<input type="checkbox"/>	RE	Restricted to a group specified by the consortium
<input type="checkbox"/>	CO	Confidential, only for members of the consortium

Table of Contents

1	<i>Introduction</i>	3
2	<i>Past events – Storyline foundations</i>	5
2.1	Storm Xynthia	5
2.2	Storm Xaver.....	6
2.3	Coastal flooding in Emilia-Romagna	7
3	<i>Methodology</i>	9
3.1	Extreme sea-level modelling.....	9
3.2	Inundation modelling	10
3.3	Impact assessment.....	13
3.3.1	Selection and collection of critical infrastructure assets	13
3.3.2	Asset damages to critical infrastructure	14
3.3.2.1	Energy	15
3.3.2.2	Transportation.....	16
3.3.2.3	Telecommunication	17
3.3.2.4	Waste	17
3.3.2.5	Water.....	18
3.3.2.6	Education.....	18
3.3.2.7	Health.....	19
3.3.3	Wider economic impacts of infrastructure failure	19
3.3.3.1	Macroeconomic model.....	19
3.3.3.2	Coupling infrastructure failure to economic impacts	20
4	<i>Storylines</i>	21
4.1	Storm Xynthia	21
4.1.1	Extreme sea-level and coastal inundation.....	21
4.1.2	Asset damage to critical infrastructure.....	23
4.1.3	Wider economic impacts of infrastructure failure	25
4.2	Storm Xaver.....	27
4.2.1	Extreme sea-level and coastal inundation.....	27
4.2.2	Asset damage to critical infrastructure.....	28
4.2.3	Wider economic impacts of infrastructure failure	30
4.3	November 2002 Storm Surge in Emilia-Romagna	31
4.3.1	Extreme sea-level and coastal inundation.....	31
4.3.2	Asset damage to critical infrastructure.....	33
4.3.3	Wider economic impacts of infrastructure failure	35

5 Discussion.....36
6 Concluding remarks and next steps.....37
7 Bibliography.....39



1 Introduction

Flooding is the most damaging natural disaster in the world, causing global losses more than ~USD100bn in 2017 alone (Munich RE, 2017). Global warming and the remote melting of the ice-sheets of Greenland and Antarctica will further increase the frequency and severity of flood hazards of European coastal regions, its people and economic assets. Moreover, flood risk will increase due to the continuous exposure of people and assets in Europe's coastal regions, which is expected to grow by a factor of two by 2050 (ECA, 2018).

When focusing on Europe's coastal infrastructure, a recent report by the European Environment Agency (EEA, 2017) states that port facilities and critical infrastructure networks are particularly vulnerable to flooding and erosion (Forzieri et al., 2017). General climate change losses to critical infrastructure would by 2100 amount to more than 10 times the present damage of €3.4 billion per year, only due to climate change. Critical infrastructure is important for the continuity of vital societal functions and is commonly associated with facilities such as the electricity grid, (tele)communication, transport, gas and water treatment plants. Ports are important hubs for the economy and serve as a crucial link in global trade relations. Furthermore, protective infrastructures (e.g., levees, dams, and managed dunes and beaches) are essential as well to reduce the risk from flooding.

This report provides the building block for assessing event-based storylines with respect to the impact of coastal flooding in Europe to critical infrastructure. We develop the definitions of Sillmann et al (2021) and Shepherd et al. (2018), to define storylines as "self-consistent unfolding of past events, or of plausible future events, and society in which they occur". In this context, we sketch a sequence of events with an underlying causal relationship that forms a logical narrative linking climate hazards at a given location in the world to a socio-economic impact on the European continent. In this report, we focus on the impact of remote climate drivers on sea-level rise and its impact on coastal flood risks.

We assess the direct and indirect impacts of three storylines in the present-day climate ("the past") with respect to coastal flooding. These storylines will be further explored in future climate situations in the upcoming deliverable D7.4. As such, this report primarily explains and develops the different modelling steps that are required to estimate the quantitative impacts of storylines with respect to climate impacts to infrastructure along the European coast. To assess the present-day condition of these storylines, we start with the estimation of extreme sea-levels as a result of three specific storms, followed by an inundation modelling exercise to estimate inundation levels along the coastline. Using these inundation maps, we can estimate the direct

asset damage to critical infrastructure along the coast and the indirect economic impacts as a result of the failure of this infrastructure.

The remainder of this report is structured as follows. Chapter 2 provides a description of the past events that will provide the foundation of our storylines that will be further developed in this report. Chapter 3 explains the method in detail. Chapter 4 presents the quantitative outcomes of the three storylines. In Chapter 5, we discuss the results and our approach. Finally, Chapter 6 concludes our findings.

2 Past events – Storyline foundations

2.1 Storm Xynthia

Storm Xynthia was a severe windstorm which crossed Western Europe between 27 February and 1 March 2010, causing casualties and major damage in multiple countries. The storm started as a depression over the Atlantic Ocean (on 23 February 2010) and subsequently developed under supportive climatic conditions into a heavy storm. Storm Xynthia made landfall along the coast of France during the night of 28 February, continued its path in a northeast direction, and eventually faded out over the southern Baltic Sea within a time span of 24 hours (Figure 1).



Figure 1. The course of storm Xynthia, which started in the Atlantic Ocean and moved from southwest to northeast over Western Europe. Adapted from Kolen, B., et al. (2010)

The storm led to coastal floods, with the coastal areas of the Vendée and Charente-Maritime in France particularly hard-hit. Intense wind gusts were measured along the Western Coast of France, in places reaching wind-force 10 (of 12) on the Beaufort scale, which is categorized as a 'storm force gale'. Wind gusts of approximately 160 km/h were detected at the island Île de Ré and the department Deux-Sèvres, and 130 km/h at stations in the coastal towns La Rochelle and Les Sables-d'Olonne. The combination of storm surge, a high tide and wave setup resulted in high water levels, with the highest water level of 4.5 metres NGF (General Levelling of France) measured at La Rochelle (Kolen et al., 2010).

An area of more than 50.000 ha was flooded causing 47 fatalities in Vendée and Charente-Maritime (Kolen et al., 2013). The storm resulted in widespread material damage to houses, (agricultural) businesses, and infrastructure. Major power failures left 1 million households without power services (that lasted at least 12 hours in some areas); boats, pontoons and landings in flooded harbors were destroyed; and the coastal railway between La Rochelle and

Rochefort was shut down for several weeks. Multiple flood defences failed, including seven dike locations in Gironde (Kolen et al., 2013), while other flood defences along the coast were damaged due to overtopping and erosion processes (Kolen et al., 2010). The damage in France caused by the storm is estimated to be around 1.5 billion euros, of which 700 million is attributed to flooding (Chauveau et al., 2011).

2.2 Storm Xaver

In early December 2013, storm Xaver, a severe winter storm, moved across northern Europe. A low-pressure system formed from a warm front wave over the North Atlantic south of Greenland on 4 December 2013, which rapidly evolved into a winter storm (Deutschländer et al., 2013). Whereas the majority of storms during the 2013-2014 winter season were losing intensity by the time they made landfall, Xaver continued to strengthen after crossing the British Isles into the North Sea driving strong winds and a storm surge across mainland Europe (RMS, 2014). Xaver crossed Northern Europe on 5 and 6 December 2013, with high wind speeds (e.g., 160 km/h in Germany, hurricane force 12 on the Beaufort scale (Deutschländer et al., 2013)). The pathway of Xaver over northern Europe and the maximum storm surges it induced across the coastline of the North Sea region are presented in Figure 2.



Figure 2. The course of winter storm Xaver over northern Europe, moving from northwest to southeast. The maximum surges due to the storm are presented for multiple locations along the coastline of the North Sea region. Adapted from RMS (2014).

Compared to the infamous and severe 1953 storm (when around 2200 people lost their lives across the North Sea region), storm Xaver had a smaller surge but coincided with a larger

astronomical tide. This coincide of astronomical and meteorological drivers results in a much greater length of coastline experiencing extreme high-water levels (higher than in 1953) (Wadey et al., 2015). Flood barriers in different countries had closed their gates to protect areas behind the barriers from flooding. For example, the Netherlands closed the Eastern Scheldt storm surge barrier, and flood gates to protect Hamburg were activated as well (Spencer et al., 2015). On 6 December 2013, the Thames Barrier experienced the highest water levels since its completion in 1982 and was kept closed for two consecutive days (Wadey et al., 2015).

The flood defenses, developments in forecasting, and improved risk management systems (e.g., warning systems, evacuation plans) prevented the high death toll that was experienced during a similar storm surge in 1953 (RMS, 2014; Spencer et al., 2015). However, storm Xaver was one of the costliest storms to hit Europe: insured losses are estimated to be in the range of 1.4-1.9 billion euros (Wadey et al., 2015), while economic losses are expected to be even higher (Rucinska, 2019). Record-breaking water levels were measured along large parts of the German Bight coastline on 6 December 2013 (Dangendorf et al., 2016). The port city of Hamburg measured a storm surge of 6.09m above mean sea level, yet which led to flooding in only some parts of the city (proving the effectiveness of the flood protection structures) (RMS, 2014). Large-scale power outages (mostly wind-triggered) occurred in the UK, Ireland, Poland, southern Sweden, and areas of Northern Germany (Kettle, 2020). Port operations were interrupted, off-shore wind farms were shut down, and flight and rail services suspended.

2.3 Coastal flooding in Emilia-Romagna

In 2002, a succession of storms resulted in a series of extreme sea level events between November 14 and November 19 along the North Adriatic coast of Italy. The coastal area of the Emilia-Romagna Region was particularly hard hit, with significant wave heights of about 4.70 m (with a N-NE direction) registered close to the municipalities of Rimini and Cesenatico. Both flooding and erosion resulted. Coastal flooding occurred in Rimini, Cesenatico, and Marina di Ravenna, with erosion taking place along the Riminese coast and to the south of the Po Delta (Figure 3).

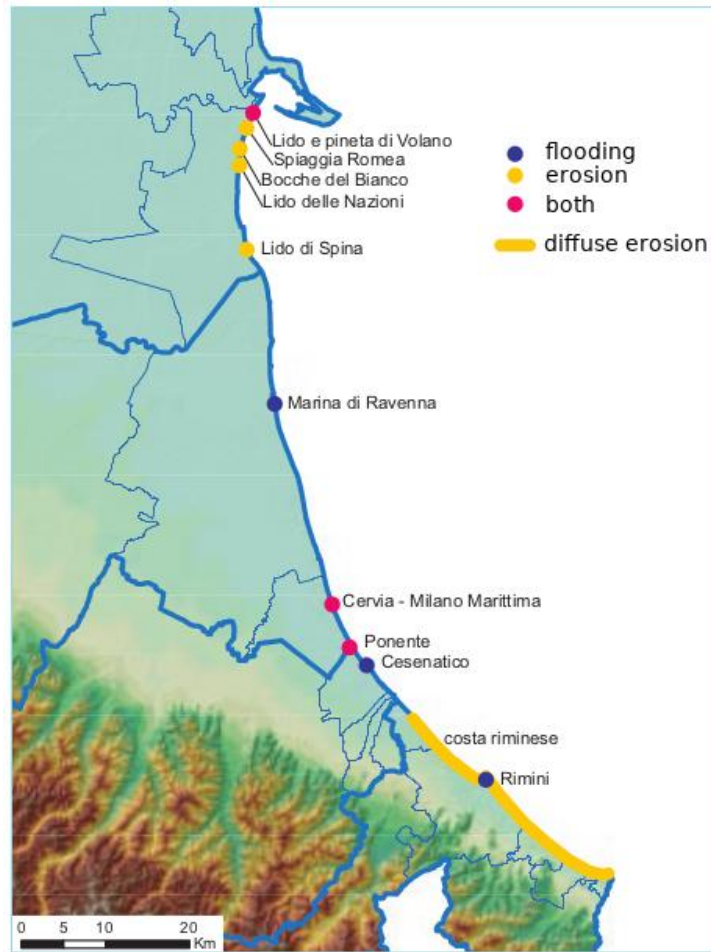


Figure 3. List of locations hit by and the main consequences due to the extreme sea level events between 14-19 November of 2002. Adapted from Perini et al., 2011.

November 2002 was characterized by an exceptionally intense low-pressure system over the Mediterranean that led to numerous meteorological anomalies, including intense rainfall associated with river floods and abnormal sea level pressure leading to coastal flooding events. The persistence of strong *sirocco* (i.e. south-westerly) winds across the central Mediterranean, particularly on the Adriatic Sea, led to numerous storm surge events that severely hit the coasts of Emilia-Romagna. The worst coastal flooding episodes were registered between 14 and 19 November, when a five consecutive days storm was associated with one of the highest water levels ever recorded in the region (Perini et al., 2011).

Damage to buildings and infrastructure was reported by the Emilia-Romagna regional administration, and some municipalities and locations requested that a state of calamity be declared. The Rimini coastline was severely damaged by the event. There were damage reports to the coastal defense structures and buildings, and 12,000 tons of material has been accumulated along the Riminese coastline. The ports of Riccione and Bellariagea Marina required emergency dredging. Approximately one million euros have been allocated for

interventions such as cleaning and nourishment of critical points along the coast of Emilia-Romagna following the events between 14 and 19 November (Perini et al., 2011).

3 Methodology

3.1 Extreme sea-level modelling

Extreme sea level conditions for the storms of Xaver and Xynthia are modelled using the Global Tide and Surge Model v3.0 (GTSMv3.0). GTSMv3.0 is a depth-averaged hydrodynamic model with global coverage that dynamically simulates tides and storm surges. The model has global coverage and is forced by the tide-generating forces and external forcing fields (e.g. winds, surface pressure). The uniform bottom friction coefficient and internal wave drag coefficient have been tuned to match observed total rates of energy dissipation. For surges, the relation by Charnock (1955) to model the wind stress at the ocean surface is used, and the drag coefficient has also been tuned during the calibration process. For this report, we use a GTSM reanalysis dataset that was computed by forcing the model with the newly available ERA-5 reanalysis. This dataset provides information on real historical water-levels that we use to model Xynthia and Xaver. The time-coverage of this dataset is 1979-2017 (Muis et al., 2016).

GTSM is a free-running model without assimilation of observed tides or surges that constrains the solution. It uses the unstructured model Delft3D-FM (Kernkamp et al. 2011) to employ a flexible distribution of resolution, which results in high local accuracy at a lower computational cost. It has a 1.25km coastal resolution in Europe. The resolution decreases from the coast to the deep ocean to a maximum of 25km. Increased resolution has also been added in the deep ocean with steep topography areas to enable the dissipation of barotropic energy through generation of internal tides. The bathymetry used consists of a combination of EMODnet high-resolution (250m) bathymetry for Europe from:

<http://www.emodnet.eu/bathymetry>

and corrected for LAT-MSL differences and General Bathymetric Chart of the Ocean 2014 (GEBCO 2014, <https://www.gebco.net/>) with a 30 arc seconds resolution available from:

<https://cds.climate.copernicus.eu/cdsapp#!/dataset/sis-water-level-change-timeseries?tab=overview> with DOI: 10.24381/cds.8c59054f.

For the case of Emilia-Romagna, we use detailed historical data of the extreme sea level as available from regional studies and post-event reports (ISPRA, 2005; Perini et al., 2011) to calibrate the flood inundation model. Two tide gauges along the coastline of the Emilia-Romagna region are of particular interest for characterizing the storm surge event, namely the station of Ancora (Mar1) and the Punta della Maestra (Emi1). We obtain historical data on sea

level height, maximum wave height, wave period, and wave direction for the November 2002 event from the regional catalog of extreme sea level (ISPRA, 2005). Information is collected for the extreme sea level events between the 14th and 19th of November 2002. As per the other case studies (i.e., Storm Xaver and Storm Xynthia), we will use GTSM data for simulating coastal inundation under future climate periods.

3.2 Inundation modelling

To estimate coastal flood maps for our storylines, we use the ANUGA model, developed by the Australian National University (ANU) in collaboration with Geoscience Australia (GA). ANUGA is a 2D-Hydrodynamic model capable of simulating the free surface elevation of water flow over land areas. The model simulates the wetting and drying of land areas, thus being suitable for simulating coastal inundation over dry land and around/above structures, such as buildings and flood defence structures (Roberts, et al. 2015). The fluid dynamics in ANUGA are based on a finite-volume method for solving the shallow water wave equations, being based on continuity and simplified momentum equations (Zoppou and Roberts 1999). ANUGA uses an irregular triangular grid, thus allowing the use of coarser or finer grids over specific areas and potentially providing more accurate spatial representation of the 2D domain. For each triangular element and time step, the model computes the:

- Water surface level;
- Bed elevation (and depth), and;
- Horizontal (x and y) momentum.

The initial conditions at every mesh point of the ANUGA model are the bed elevation, the friction (Manning friction coefficient, a forcing term), and the water stage (height of water surface). The boundary conditions of the ANUGA model can be selected from the following options (Roberts, et al. 2015):

- Reflective boundary: Returns same stage as in its neighbour volume but momentum vector reversed 180 degrees (reflected). A reflective boundary condition models a solid wall.
- Transmissive boundary: Returns same conserved quantities as those present in its neighbour volume. This is one way of modelling outflow from a domain.
- Dirichlet boundary: Specifies constant values for water level, and x- and y-momentum at the boundary.
- Time boundary: Like a Dirichlet boundary but with behaviour varying with time.

We use a high-resolution Digital Elevation Model (DEM) and bathymetry data to characterise the bed elevation in the ANUGA domain. Bathymetry data is obtained from EMODnet 2018 at a grid resolution of 1/16 arc minutes (approximately 115m), while the base DEM used is the high-accuracy CoastalDEM for coastal areas, at 90m resolution. Coastal defences such as dykes and sea walls are obtained from OpenStreetMap (OSM). We define the area of interest

represented in ANUGA according to the extension of the storm surge event of interest and the availability of data from GTSM. For instance, for the Xaver storm, we include a large portion of the German coast in the North Sea, from Husum to the north to Emden to the south-west. We split the domain into areas of different modelling resolution, characterised by finer or coarser triangular elements according to the presence of coastal defence structures or exposed elements. Higher resolution areas (i.e. triangular elements of about 90m²) are defined for areas where a complex water dynamic is important (e.g. overtopping of coastal defence structures), while lower resolution areas are defined for non-relevant areas (e.g. areas above 15m in elevation) or areas where water flow dynamics is simple (e.g. open sea way from the coastline). An example of such a setup is shown in Figure 4, for the Xaver storm, in Northern Germany.

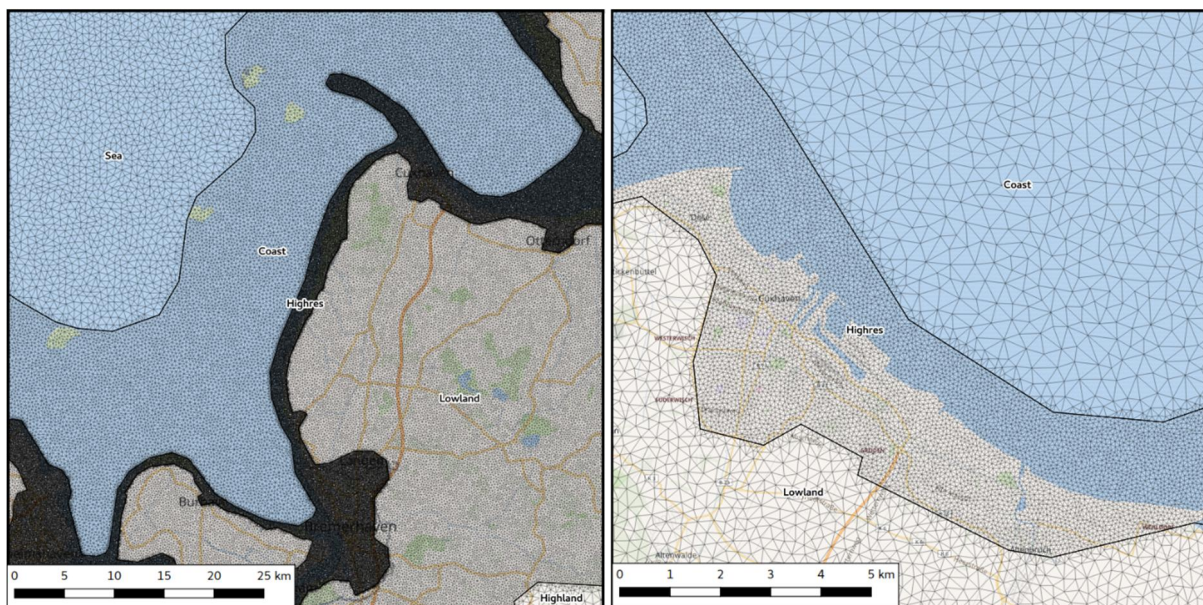


Figure 4. Example of an irregular triangular mesh in ANUGA generated for simulating the Xaver storm in Northern Germany. On the left, an overview of the triangular mesh at the coastline between the Weser and Elbe rivers. On the right, a zoom-in over the city of Cuxhaven.

The triangular elements in Figure 4 are represented as the polygons in black. The number of triangles considered in this application are above 1 million elements, most of which are concentrated in the high-resolution area along the coastline and covering the main dykes/seawalls in the area. Due to the higher concentration of triangular elements along the coastline, individual triangular elements cannot be identified, thus looking like a darker region. Individual triangular elements can be seen on the open sea to the upper-left of the figure. The initial conditions for every triangular element in ANUGA are set-up according to the water level in GTSM at the beginning of an event of interest (e.g. storm Xaver), and the simulation is run for the total duration of the event. The boundary conditions of ANUGA are setup according to GTSM and are forced with water level data from GTSM. Momentum data is manually

calibrated to emulate the storm surge wave propagation inside the model's domain. For instance, if an event is moving south-west to north-east, the boundary conditions in ANUGA are set-up in such a way that the water flow entering the domain accounts for these dynamics. This setup allows for the numerical simulation of the propagation of flood waves and inland inundation. An example of the setup of boundary conditions and the resulting momentum is shown in Figure 5, for the Xynthia storm, in Western France.

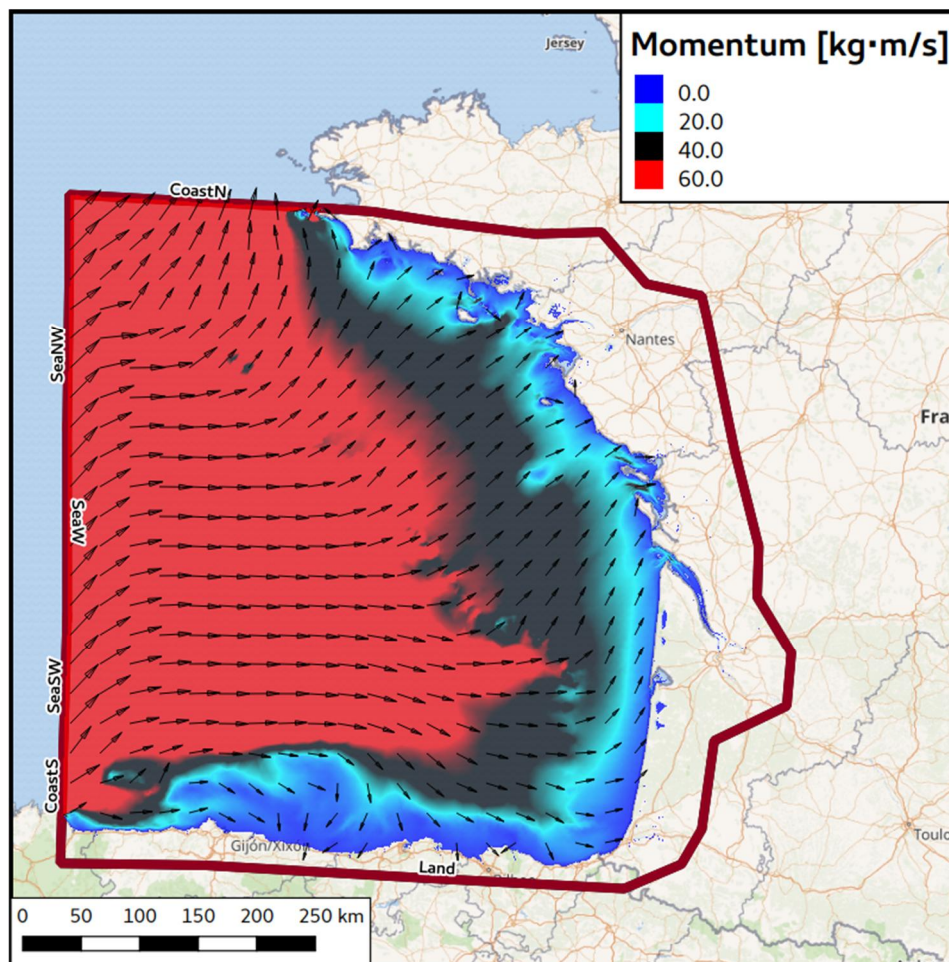


Figure 5. Example of boundary conditions and the resulting momentum in ANUGA's domain for simulating the Xynthia storm in Western France.

ANUGA allows for accounting for the presence of coastal defence structures. In particular, the model allows for simulating the dynamics of coastal defence structures by allowing the modification of the bed elevation. This is particularly useful when simulating the activation of mobile gate systems (e.g., as the *Porte Vinciane*, a mobile gate system in Cesenatico, in Italy) or dam/dyke breaks (e.g., during the Xynthia storm in Western France, the sea wall in the coastal town of L'Aiguillon-sur-Mer was smashed down, leading to a more intense flood hazard in the area). By considering not only the presence but also the dynamics of coastal flood defences, ANUGA allows for producing the flood extent, water depth and momentum at

every time step of a particular flood event. The output maps of the inundation modeling are, then, projected on a high-resolution regular grid.

3.3 Impact assessment

3.3.1 Selection and collection of critical infrastructure assets

For this analysis, we represent the infrastructure network by seven overarching Critical Infrastructure (CI) systems: *energy*, *transportation*, *telecommunication*, *water*, *waste*, *education*, and *health*. This is in line with the classification of infrastructure systems discussed in literature, whereby CI related to health and education have been receiving increasing attention. We use OpenStreetMap (OSM) to extract relevant infrastructure types, where we apply a combination of 97 active OSM tags to represent 42 infrastructure types that are categorized under the seven overarching CI systems. Table 1 provides an overview of the 41 infrastructure types and its categorization that are considered in this study.

Table 1. List of infrastructure types considered in this study, categorized under ten CI subsystems and seven overarching CI systems.

System	Subsystem	Infrastructure type	System	Subsystem	Infrastructure type
Energy	Power	<ul style="list-style-type: none"> • Cable • Line • Minor line • Plant • Substation • Power tower • Power pole 	Water	Water supply	<ul style="list-style-type: none"> • Water tower • Waster well • Reservoir (covered) • Water works
Transportation	Railways	<ul style="list-style-type: none"> • Railway 	Health	Healthcare	<ul style="list-style-type: none"> • Clinic • Doctors • Hospital • Dentist • Pharmacy • Physiotherapist • Alternative Laboratory • Optometrist • Rehabilitation • Blood donation • Birthing centre
	Roads	<ul style="list-style-type: none"> • Motorway • Trunk • Primary • Secondary • Tertiary • Other 			
	Airports	<ul style="list-style-type: none"> • Airport 			
Telecommunication	Telecom	<ul style="list-style-type: none"> • Communication tower • Mast 			
Waste	Solid waste	<ul style="list-style-type: none"> • Landfill • Waste transfer station 	Education	Education	<ul style="list-style-type: none"> • College • Kindergarten • Library • School • University
	Water waste	<ul style="list-style-type: none"> • Water waste treatment plant 			

The geospatial information on CI that we extract from the publicly available OSM dataset is stored in three different datatype formats: *point*, *line* and *polygon* (Figure 6). Firstly, a *point* feature represents a specific point in space and is defined by its latitude and longitude. Telecommunication towers, for example, are stored as *point* features in OSM. Secondly, a *line* feature is a segment that is connected by two or more-point features. Linear infrastructures such as roads and cables are stored under the *line* datatype format. Lastly, a *polygon* feature is represented by a connection of line features, whereby the last point is connected to the beginning. Infrastructure types as hospitals, universities and airports are stored as polygons.

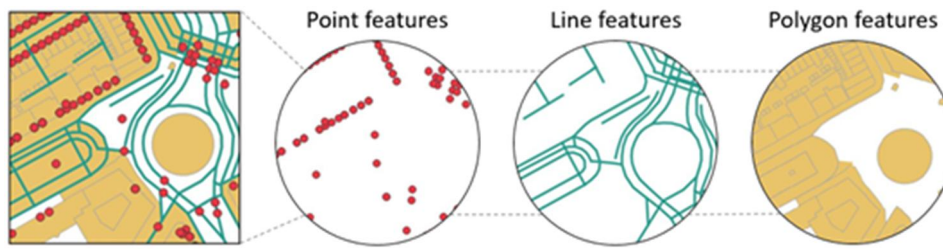


Figure 6. Visualization of raw Open Street Map data of a given area, with a breakdown by the datatypes. Adapted from Nirandjan, et al. (under review).

3.3.2 Asset damages to critical infrastructure

To assess the direct damages to infrastructure assets, we follow a traditional damage assessment approach, in which we combine the geospatial information of the infrastructure assets (Section 3.3.1) with flood hazard data on inundation levels and extent (Section 3.2), and vulnerability data.

As the CI dataset consists of three different datatypes (see Section 3.3.1), three approaches to process these datatypes are developed accordingly. For all datatypes we apply the same principle, whereby we use the geospatial location of the infrastructure asset to detect whether the asset is located in an inundated area. If so, the inundation depth(s) for the specific location(s) is adapted and combined with vulnerability data to calculate the asset damage. To process the damage for inundated point features, this means that the asset under consideration falls within the boundaries of one specific inundation cell that represents one particular inundation level. This specific inundation level is then combined with vulnerability data at asset level. However, this is different for line and polygon features as one asset can be present in multiple inundation cells. For inundated line features, we therefore calculate the length (in meters) of a linear asset (e.g. primary road) per inundation cell that overlaps with the linear asset. The exposed length is then combined with the inundation level of the given inundation cell and vulnerability data that holds potential damages per exposed meter. For polygon features, we calculate the inundated area (in square meters) per inundation cell that overlaps with the polygon asset (e.g. hospital). Subsequently, the exposed area is then combined with the inundation level of the given inundation cell and vulnerability data that holds potential damages per (1) exposed square meter, or (2) per facility for a given infrastructure type. In the latter case, we disaggregate the maximum damage that may occur to an asset in its whole (e.g. power plant) to the potential maximum damage that may occur per square meter.

The potential direct damage to CI is estimated through the use of vulnerability curves (also known as depth-damage or stage-damage curves). We collected data on the vulnerability of CI and developed a database of vulnerability curves that show the relation between the

intensity of the hazard (inundation levels of the flood) and the potential damage to a specific infrastructure type. Potential damage can either be expressed in absolute values, or in relative numbers (e.g., 0 – 100% damage). We expressed the potential damage in relative numbers as a function of water depth and use it with maximum damage values to estimate the potential damage in euros for a specific asset (reference year 2015) that experiences a certain level of inundation. It is common practice to apply maximum damages that are based on construction costs. We use construction costs derived from literature for infrastructure types that lack specific data on maximum damages that can be used directly for risk assessments. Hereby, we assume that the costs for reconstruction are 60% of the construction costs (e.g., Huizinga et al., 2017). In the following subsections (3.3.2.1-3.3.2.7), the vulnerability of the infrastructure types per CI system is discussed in further detail.

3.3.2.1 Energy

Hazard United States (HAZUS) is a geographic information system-based tool for analyzing natural hazard risk, which is developed and freely distributed by the Federal Emergency Management Agency (FEMA). Specifically, for flood risk, FEMA developed a technical manual that contains vulnerability information for various types of infrastructure. We apply the vulnerability curves and maximum damages for plants and substations developed by FEMA (2013).

We distinguish between lines and minor lines, whereby OSM categorizes lines as high-voltage overhead powerlines that are usually supported by towers or pylons, while minor lines are supported by poles used for low-voltage transmission. We use a vulnerability curve for overhead transmission and distribution (T&D) systems, which assumes that only little damage occurs due to flooding (FEMA, 2013; Miyamoto, 2019). Maximum damages were not provided by either FEMA (2013) and Miyamoto (2019). We therefore base our maximum damages on construction costs for overhead lines in urban (for lines) and rural (for minor lines) areas provided by Hall (2009). We also conduct the construction costs for underground cables from Hall (2009). Based on a survey conducted by Burns & McDonnell (n.d.), underground cables are not likely to suffer direct damage due to flooding. Flooding impacts the above grade equipment that the cables are connected with, and this failure may propagate into the whole energy circuit. This finding is also supported by Hall (2009). However, uprooting of trees (Hall, 2009) and soil liquefaction (Miyamoto, 2019) may cause damages to underground infrastructure. For this study, we assume that no damage occurs to underground cables due to flooding as we assume a relative low flow velocity.

For the power towers and power poles we apply the vulnerability curve for T&D systems. Again, maximum damages were not provided, and we therefore use construction costs for power towers and poles. Midcontinent Interdependent System Operator (MISO) provides yearly

reports with estimated costs for various energy assets, including power towers and poles. OSM describes power towers as assets that carry high-voltage overhead power lines, and are often constructed from steel, while power poles are often made from wood. For this reason, we use the construction costs for single- and double circuit steel towers built for a range of high-voltage overhead lines for determining the maximum damage for power towers, while we only use construction costs for wooden poles (single and double circuit) for determining the maximum damage for power poles.

3.3.2.2 Transportation

Huizinga et al. (2017) provides grid-based vulnerability curves for application to the road network that can be used in combination with maximum damages in euro/m². A recently published article, which assesses the flood risk of the European network, made an object-based translation of these vulnerability data (van Ginkel et al., 2021). As part of this assessment, van Ginkel (2021) calculated the maximum damage in millions of euros per kilometer for the infrastructure types: motorway, trunk, primary, secondary, tertiary, and other. The maximum damages are derived by multiplying the maximum damage per m² provided by Huizinga et al. (2017) with estimated typical roads width per road type. We use the vulnerability curve provided by Huizinga et al. (2017) for the road network in combination with the maximum damages in length units for different road types proposed by van Ginkel et al. (2021).

The vulnerability function is based on Kellerman et al. (2015). Instead of a curve, they propose a staircase threshold-wise damage states to present the vulnerability of railways, whereby three stages of damage are classified. The railways are assumed to be a standard double-tracked railway cross-section that consists of the following elements: substructure, superstructure, catenary and signals. The first damage class relates to the substructure of the railway that is (partly) impounded by water but results in only little damage. The second damage class assumes that the substructure and superstructure of a track segment is completely flooded, which is expected to result in damage to at least the substructure. The final class assumes damage to the superstructure, catenary and/or signals, and that complete restoration is needed for the standard cross-section of the affected track segment. The maximum damage for railways is based on construction costs for railways (diesel and electrified) that are proposed by Carruthers (2013).

Lastly, a vulnerability curve for airports is provided by Kok et al. (2005). They also provide a maximum damage value given in damage per exposed footprint of an airport (euro/m²). The usage of this in combination with the spatial airport data, which are extracted from OSM in polygon format, may lead to an overestimation of the direct damages to airports. These polygons represent the airports as a whole, including areas that are covered by structural components, but also areas that are less important for risk analysis (e.g., grass). We therefore

decide to break down the direct damages to airports by presenting structural damages to terminals and runways. For terminals, we use the vulnerability curve of Kok et al. (2005) in combination with maximum damage based on construction costs estimated by Carruthers (2013). Due to absence of more specific vulnerability curves for runways, we apply the vulnerability curve of Huizinga et al. (2017) estimated for roads. The maximum damages are based on construction costs for runway types made of concrete and asphalt (Gibson et al., 2011).

3.3.2.3 Telecommunication

The infrastructure types communication tower and mast represent the system 'telecommunication'. More specific vulnerability data for telecom assets are still lacking in the current body of literature. Therefore, we apply the vulnerability curve for the power systems to telecom infrastructure, which has also been done in Kok et al. (2005).

Communication towers are structures with greater heights (could be above 100m) and are used for transmitting a range of radio applications (e.g. television, radio, mobile phone). Communication towers are often made from concrete. In contrast, masts are usually smaller, narrow structures only a few meters high, and are typically used for a single radio application. We use the vulnerability curve of FEMA (2013) that we also apply for large power towers for communication towers. We assume that only little damage occurs to large communication towers, and this is what this vulnerability curve embodies. We used this in combination with maximum damages for 'other community facility' provided by FEMA (2013) as no specific construction cost data were available for communication towers. On the other hand, we assume that masts are more vulnerable to flooding as they are smaller structures compared to communication towers. We therefore apply the vulnerability curve proposed by Kok et al. (2015) for electricity and communication systems, which assumes higher damage factors. The maximum damage of masts is based on construction costs provided by Foster (2015) and Liebman (2018).

3.3.2.4 Waste

The waste system is subdivided into two subsystems: solid waste and water waste. The solid waste subsystem is represented by infrastructure types waste transfer station and landfill, whereas the water waste subsystem is represented by water waste treatment plants.

In the current body of literature, specific vulnerability data on the solid waste infrastructure types is still lacking. We therefore apply the vulnerability curve and maximum damage proposed by Huizinga et al. (2017) for industrial areas. Waste transfer stations are extracted from OSM as polygon data, and the maximum damage is given in damage per exposed footprint. Landfills are excluded from the direct risk assessment but are included in the

development of the CISI (see section 3.3.3.1). On the other hand, we use vulnerability curves and maximum damage estimates specifically developed for water waste treatment plants provided by FEMA (2013). This vulnerability data assumes that minor cleanup and repair activities are required when flood level exceeds ground level, and major activities when inundation levels reach approximately 1 meter.

3.3.2.5 Water

The water system is represented by four infrastructure types, namely water tower, water well, reservoir covered, and water works. We apply vulnerability data provided by FEMA (2013) on the four infrastructure types. FEMA (2013) includes vulnerability curves and maximum damages for (potable) water systems.

The infrastructure type reservoir covered are large man-made tanks for holding water. FEMA (2013) provides vulnerability data for storage tanks at ground level, elevated structures, and tanks that are below ground level. However, OSM does not specify the height of the assets. We therefore take the average of the vulnerability curves and maximum damages for the different storage tanks specified by FEMA (2013) and apply this to the infrastructure type reservoir covered. A water tower is a structure that contains a water tank at an altitude to pressurize the water distribution network. We apply the vulnerability curve and maximum damage for elevated water storage tanks, which assumes that these structures will not be damaged during a flood. Furthermore, we use the vulnerability data specifically defined for water wells, which assumes that electrical equipment and well openings are 1 meter above ground level, and that a well is not permanently contaminated after flooding.

Water works are structures where drinking water is found and applied to the waterpipes network. The public supply of water is stored and treated in this system of buildings and pipes. The (potable) water systems section of FEMA (2013) does not specify any data on water works. We therefore use the average of the vulnerability curves and maximum damages provided for water treatment plants (open and closed structures) and apply this for water works.

3.3.2.6 Education

The education facilities are extracted from OSM as polygons. Huizinga et al. (2017) developed vulnerability data for commercial buildings, which include schools as well. We use the vulnerability curve and maximum damage specified as damage per exposed footprint (euro per m²) proposed by Huizinga et al. (2017).

3.3.2.7 Health

Health facilities are tagged in OSM as point and polygon features. We extracted both datatypes and transformed the point features into polygon features based on average health facilities footprints of the polygon features. We corrected for duplicates in the dataset by verifying whether overlaps exist between a point and polygon feature. The Huizinga et al. (2017) vulnerability data used for education facilities are applied on health facilities as well (as the category 'commercial facilities' also includes hospitals).

3.3.3 Wider economic impacts of infrastructure failure

3.3.3.1 Macroeconomic model

Over the past years, many modelling approaches have been developed (and applied) to assess the macroeconomic impacts of extreme events. This varies from more traditional Input-Output (IO) models, to various forms of Computable General Equilibrium (CGE) models (Carrera et al 2015). In addition, a wide-range of new models have been developed in recent years, such as the Acclimate model (Otto et al 2017) and the MaGE model (Fouré et al 2013). In this analysis, we will apply the Multiregional Impact Assessment (MRIA) model, developed by Koks and Thissen (2016). The MRIA model allows us to analyze the consequences within regions as well as sector-specific decreases in production capabilities that are not present in most existing IO-based models (Koks and Thissen 2016): (1) the consequences of production inefficiencies resulting from damaged industries aiming to operate at full capacity; and (2) the required increase in production in regions not affected by the direct impact to take over the production lost in the affected region (i.e. substitution). We use the MRIA model in combination with a multiregional subnational dataset for the European Union (Thissen et al 2018, 2013). This dataset consists of multiregional supply-use tables and bilateral trade between 270 European NUTS2 regions for the year 2013. A particular novelty of this approach is the high spatial resolution (NUTS2 administrative level) on a continental scale, considering not just transboundary effects between different countries, but also between regions in different countries. This allows us to capture specific trade flows that might be lost when not including interregional trade or when modelling on a country level.

Indirect economic impacts simulated by the MRIA model are estimated based on the reduction in industrial production capacities due to asset damages and flooded premises. MRIA subsequently calculates how trade flows from and to other regions change because of the flood, either positively or negatively. This trade flow change is the main driver of indirect economic effects in other regions. Negative effects occur as a result of reduced supply and demand in the affected industries of the flooded regions. Positive effects occur because industries (i.e., intermediate demand), governments and households (i.e. final demand) not

directly affected by the flood seek to satisfy, within existing trade relations, their demand for products elsewhere. In their position, agents in the model attempt to find alternative possibilities to satisfy their demand based on existing trade relations. Finally, a cascade of effects may occur when the production capacity of industries in non-flooded regions is insufficient to completely take over production from a flooded region (Koks et al., 2019a).

In line with standard input-output modelling, the MRIA model is based on the assumption of a demand-determined economy (Leontief 1951). In other words, the demand from all regions and from the rest of the world must be satisfied by the total supply in all separate regions and the rest of the world. The MRIA model is based on the region-specific technologies of industries used to make different products derived from regional technical coefficient matrices (Koks and Thissen 2016, Thissen et al 2013). Hence, the technologies can be seen as the inputs, including capital and labor, required to produce an output of different products. Products are produced at the lowest costs, and together with the demand for products in every region, these costs determine which technologies are used as well as the extent of their use. In other words, industries in the model have cost-minimizing behavior. This may mean that inefficient technologies are being used to produce products when production with the 'optimal' technology is limited due to supply constraints. To avoid extremely inefficient production in the affected region by industries that produce this product only as a by-product, it is assumed that before a region reaches its maximum regional capacity it already begins importing goods from other regions, rather than attempting to produce these goods itself. For a complete description of the model, please refer to Koks and Thissen (2016).

Ideally, modelling the macroeconomic impacts of disasters should include a temporal dimension. Unfortunately, empirical data on the dynamics of business recovery is scarce. Even more so in relation with the large uncertainty around recovery times of infrastructure failure. As such, we present the daily economic impacts for each storyline. This way the possible impacts are intuitive to interpret and can be extrapolated to certain recovery periods when more information would become available. Unfortunately, documentation is very limited with respect to post-disaster recovery of the economy. As such, recovery periods are difficult to provide.

3.3.3.2 Coupling infrastructure failure to economic impacts

For a consistent comparison between countries and regions with respect to their infrastructure density, we have developed a Critical Infrastructure Spatial Index (CISI). To generate the CISI, we translate the detailed spatial information on CI into a consistent rasterized dataset, whereby each grid cell holds information on the estimated amount of infrastructure. We created a consistent raster of the globe with a resolution of 0.1 x 0.1 degrees (approximately 11.1 x 11.1 km at the equator).

To assess the potential impact of infrastructure failure to the economy, we take multiple steps. Firstly, we overlay CISI with the inundation map of the specific storyline to analyze the potential exposure of critical infrastructure to coastal flooding. Next, we use an average depth of 0.5m of inundation and at least 50% flooded as thresholds to identify cells that may endure failure of critical infrastructure services as a result of flooding. These 'failed' cells are then overlaid with Corine Land Cover (CLC) 2018 (EEA, 2020). To estimate the potential disruption to the economy as a result of critical infrastructure failure within any NUTS2, we divide the industrial and commercial land-uses that intersects with the 'failed' cells by the total amount of industrial and commercial land-use within that NUTS2 region. This will provide us with the relative share of economic activities within a NUTS2 region that is disrupted due to critical infrastructure failure. This relative share is the input for the MRIA model to assess the wider-economic impacts.

4 Storylines

4.1 Storm Xynthia

4.1.1 Extreme sea-level and coastal inundation

The storm surge from Xynthia was mainly driven by wind-forced Ekman set-up (Bertin et al. 2012). The impact of the storm on sea level was strongly increased by coinciding with the spring tide (see Figure 7).

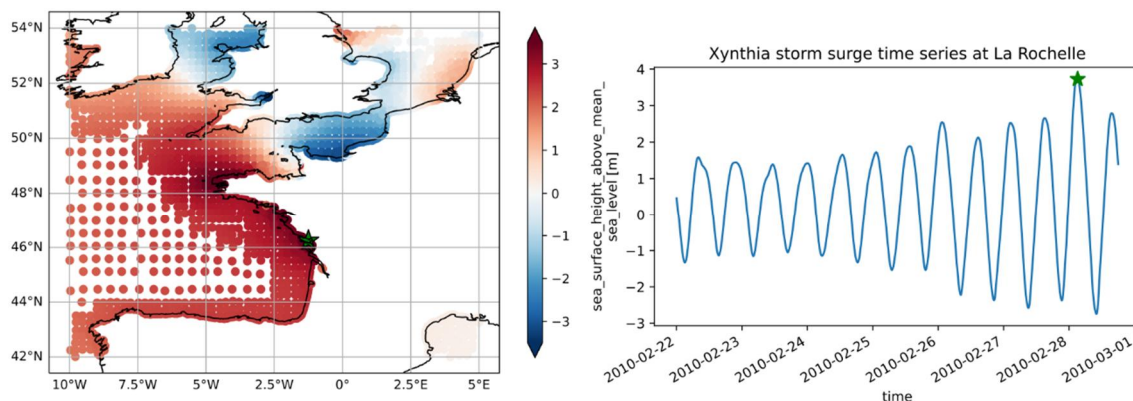


Figure 7. GTSM simulation of the influence of storm Xynthia on the sea level. Left panel: large-scale sea level condition on the 28th of February 2010 when Xynthia hit the Atlantic coast of France. Right panel: Time series of sea level before and after the storm peak (green star) in the city of La Rochelle.

The coastal inundation process was simulated using the ANUGA model. For the case of the Storm Xynthia, most of the recorded damages were caused by the rupture of seawalls and by the subsequent flooding. We incorporate such effects in our inundation modelling by considering the collapse of a seawall near the coastal town of L'Aiguillon-sur-Mer (Figure 8).

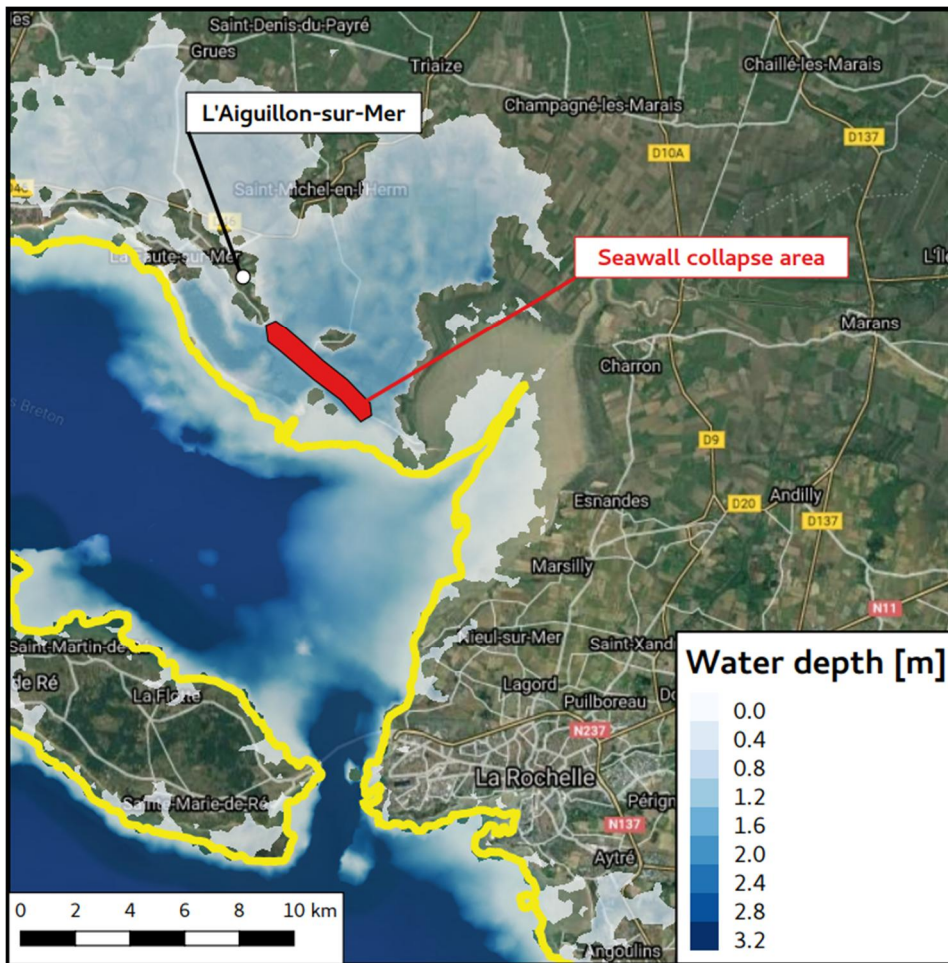


Figure 8. The consideration of a dynamic bed elevation in ANUGA allows for incorporating the seawall collapse near the city of L'Aiguillon-sur-Mer during the Storm Xynthia event. In red, the area where the seawall collapse is simulated. The yellow line indicates the coastline. Flooded areas are indicated in shades of blue, according to the water depth.

ANUGA incorporates the water level and dynamics of the Storm Xynthia from GSTM. The inundation process is designed to simulate the coastal flooding dynamics during the period with the maximum water level height of the event, thus starting on the 28th February 2010 (see Figure 7). The simulation lasts for 16 hours, thus allowing for computing the maximum coastal inundation extent. Figure 9 displays the water level distribution along the coastline of Western France as the Storm Xynthia hits the coastline. As observed (and in-line with observations and the data from GSTM), the storm peak is observed near the city of La Rochelle.

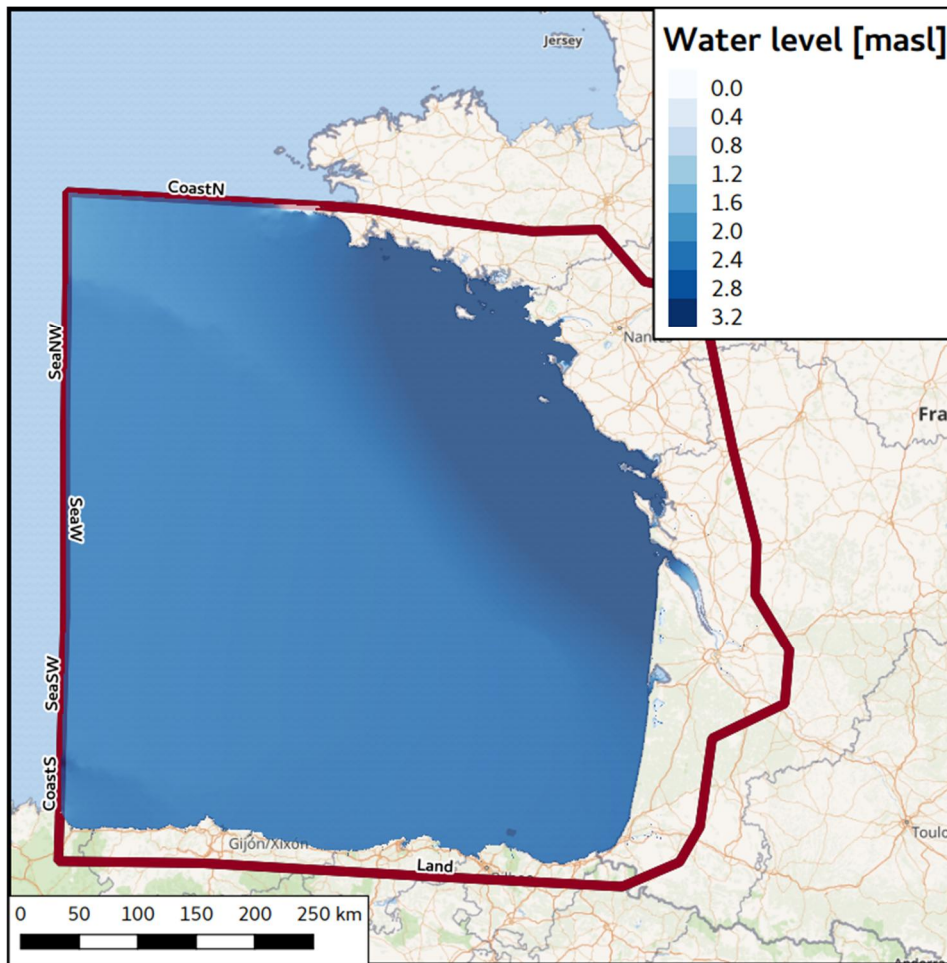


Figure 9. Storm Xynthia, as simulated by ANUGA when the storm surge hits the coast of France.

As shown in Figure 9, some flooding due to Storm Xynthia can be observed along the Atlantic coast of France. As most of the Atlantic coast of France is protected by the presence of either natural or man-made barriers, coastal flooding was observed only in localised spots, such as La Faute-sur-Mer and L’Aiguillon-sur-Mer (Chauveau et al., 2017). The simulation of the event with ANUGA correctly predicts that most of the flooded area happens near the cities of La Faute-sur-Mer and L’Aiguillon-sur-Mer, mostly due to the collapse of the seawalls, while flooding is also simulated near the city of La Tranche-sur-Mer. Significant agricultural lands in the Bay of l’Aiguillon are also simulated as flooded. The flooded areas resulting from the simulation with ANUGA are in-line with observations (Chauveau et al., 2017).

4.1.2 Asset damage to critical infrastructure

Damages to infrastructure due to storm Xynthia are widespread along the coastline of Western France. Figure 10 shows the spatial distribution of damaged infrastructure, whereby further detail of the aggregated damages is given to La Rochelle and surroundings that are particularly hard-hit.

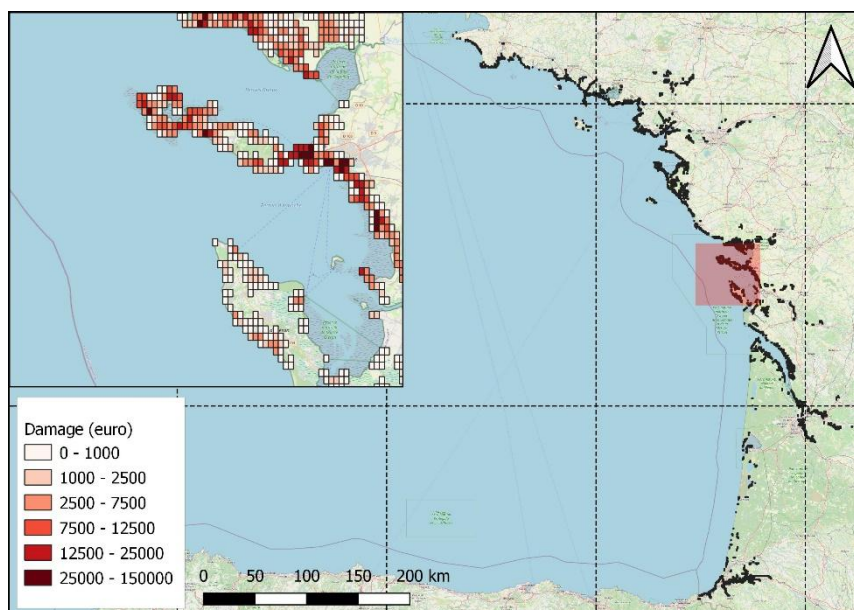


Figure 10. The spatial distribution of locations that suffer damages to critical infrastructure along the coastline of Western France due to storm Xynthia, with a detailed overview of the aggregated damages for La Rochelle and surroundings.

The total asset damage to critical infrastructure due to flooding in the coastal areas of western France is estimated to be approximately 11.3 million euros. As is shown in Figure 11, the CI system transportation has, with a damage of 6.2 million euros, the highest contribution to the total damages. The remainder of damages is due to damaged education facilities (34.2%), followed by healthcare (11.1%), waste (0.01%), telecommunication (<0.01%) and the energy system (<0.01%). The water system remains undamaged; the selected infrastructure types that represent the CI system water (see Table 1) are not located in the inundated area.

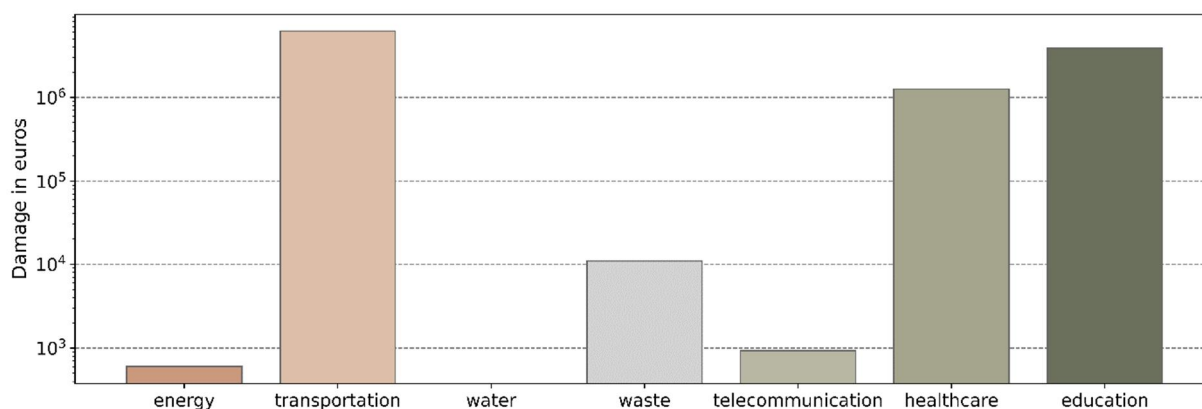


Figure 11. Damages (in euros) to critical infrastructure categorized per overarching CI system due to storm Xynthia

The relative asset damages for the 41 infrastructure types categorized per CI system are presented in Figure 12. Within the hardest-hit CI system 'transportation', the road network experiences the highest asset damages. The total damage to the road subsystem (see Table

1 for classification) amounts to 4.9 million euros, while the damage to the railway network is estimated to be 1.2 million euros. A small-scale aerodrome located near La Tranche-sur-Mer and an aerodrome on the island Île d'Yeu are (partially) flooded, resulting in a total estimated damage of 190 000 euros.

Multiple health and education facilities are exposed to flooding. Within the exposed area are 27 schools, two university buildings, two libraries, and one college that are exposed to flooding, resulting in damages of 3.2 million to school facilities and almost 700 000 euros to the other education facilities. A total of five hospitals are flooded due to storm Xynthia, which equals a damage of approximately 1 million euros. Other health facilities that are hit by the flood are rehabilitation centers, alternative health facilities, physiotherapists, doctors and pharmacies, of which the cumulative damage results in approximately 280 000 euros.

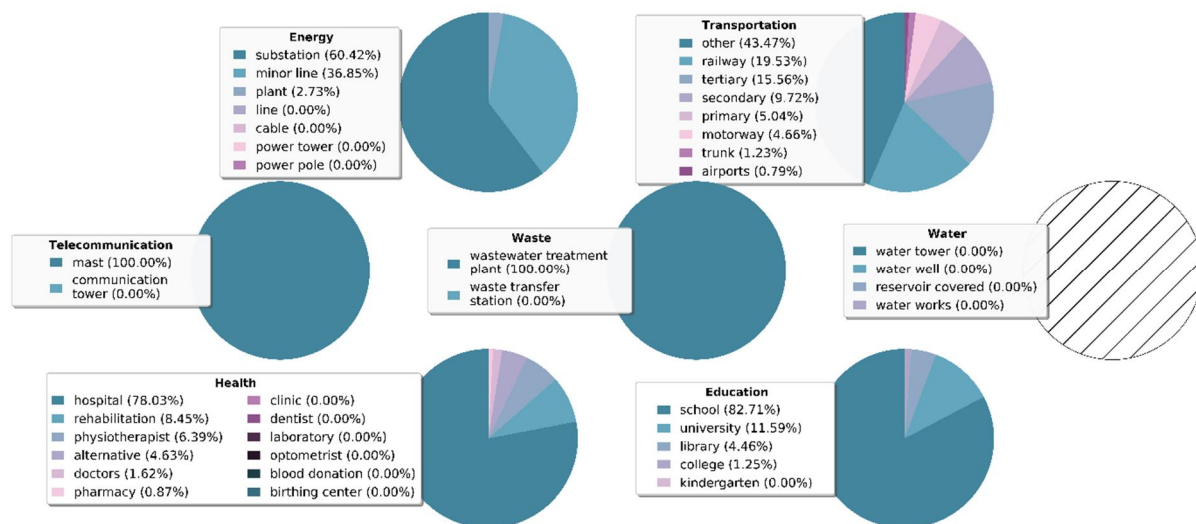


Figure 12. Relative asset damages per infrastructure type for each overarching CI system due to storm Xynthia

4.1.3 Wider economic impacts of infrastructure failure

For storm Xynthia, we have estimated an economic loss of approximately 7.2 million Euro a day for the entire European Union as a result of infrastructure failure along the French and Spanish coast due to coastal flooding. If we would only focus on the economic impacts to the affected region, the model results show a daily impact of approximately 24.3 million Euro a day. In France and Spain, the affected countries, the daily impacts amount to approximately 9.3 million Euro a day.

Figure 13 presents the relative impacts per sector in absolute and relative terms for the affected region only, the country (France and Spain in the case of Xynthia) and the wider

economic impacts to the entire European Union. In both absolute and relative terms, we find the largest economic impacts in the manufacturing sector. Interestingly, the results show a clear decrease in the absolute impacts with larger spatial scales. This indicates a clear substitution effect. While substitution is limited within the affected region (everyone is in some way affected, making it hard to take over some production), it is possible for non-affected regions to take over some of the demand and supply that is not satisfied anymore by the affected region.

This substitution effect is, however, not occurring in all sectors as pronounced as in the manufacturing sector. The wholesale and retail sectors, for example, both experience an absolute increase in impacts from country to European impacts. This indicates that other regions are also negatively affected, also outside the affected countries. A similar effect can be observed for the mining and quarrying industry. The mining and quarrying industry is worth noting, as it is not directly affected by the floods. All the impacts to this sector occur through supply chain propagations.

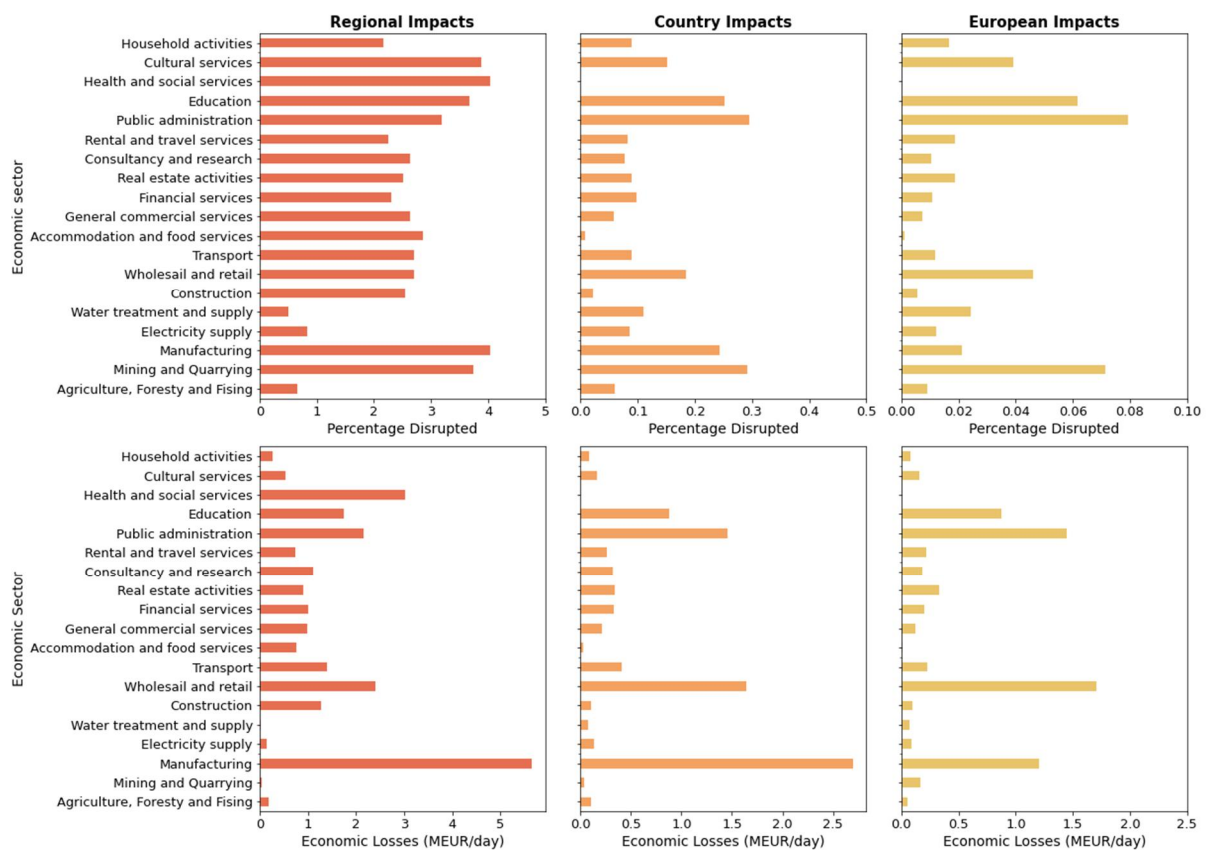


Figure 13. Daily economic impacts on a regional (directly affected regions), country (directly affected country) and European level as a result of infrastructure failure due to storm Xynthia.

4.2 Storm Xaver

4.2.1 Extreme sea-level and coastal inundation

Sea level at the German coast reached a record high during storm Xaver (see Figure 14). The peak was the result of a combination of high surge, low frequency mean sea level (hourly sea level filtered with a 14-day LOWESS) and high tide coinciding in time. While all three components were high, they were not exceptional, which means that currently observed surge, tides and mean sea level could provide a total sea level during the surge around 50cm higher than observed (Dangendorf et al. 2016). Another way to define storm surges that could have happened in the current climate, is defined by Horsburgh et al. (2021). By modifying characteristics of the pressure field of the storm (e.g. path, propagation speed, lowest pressure) they define 6 alternative physical storms, that they call “grey swans”, that would have resulted in storm surge up to 1m higher than observed.

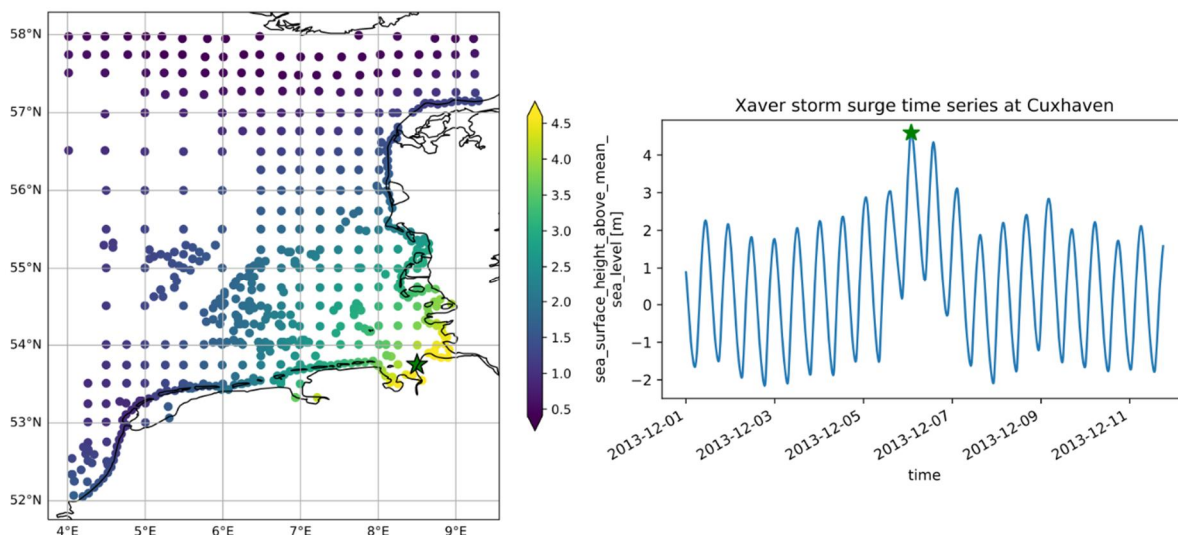


Figure 14. GTSM simulation of the influence of storm Xaver on the local sea level. Left panel: large-scale sea level condition on the 6th of December 2013 when Xaver hit the North Sea coast of Germany. Right panel: Time series of sea level before and after the storm peak (green star) in the city of Cuxhaven.

The coastal inundation process was simulated using the ANUGA model. Extreme water levels and storm dynamics of Storm Xaver are incorporated in ANUGA by using data from GTSM. The inundation process is simulated at the maximum water level height of the event, thus starting on the 6th December 2013. The simulation lasts for 16 hours. For the case of the Storm Xaver, most of the potential damages were avoided by the presence of coastal defence structures. We incorporate the presence of coastal flood defences by relying on OSM data to identify their location in space. At present, the height of primary sea dikes in the Wadden Sea region is between 6 and 9.5 m above mean sea level (CPSL, 2015). In the absence of detailed data characterising the specific height of each individual coastal defence segment, we assume a

mean height of 6.5m for the considered coastal defence structures. Figure 15 displays the water level distribution along the coastline of Northern Germany as the Storm Xaver hits the coastline. Consistent with observations and the data from GTSM, the storm peak is simulated to take place near the city of Cuxhaven.

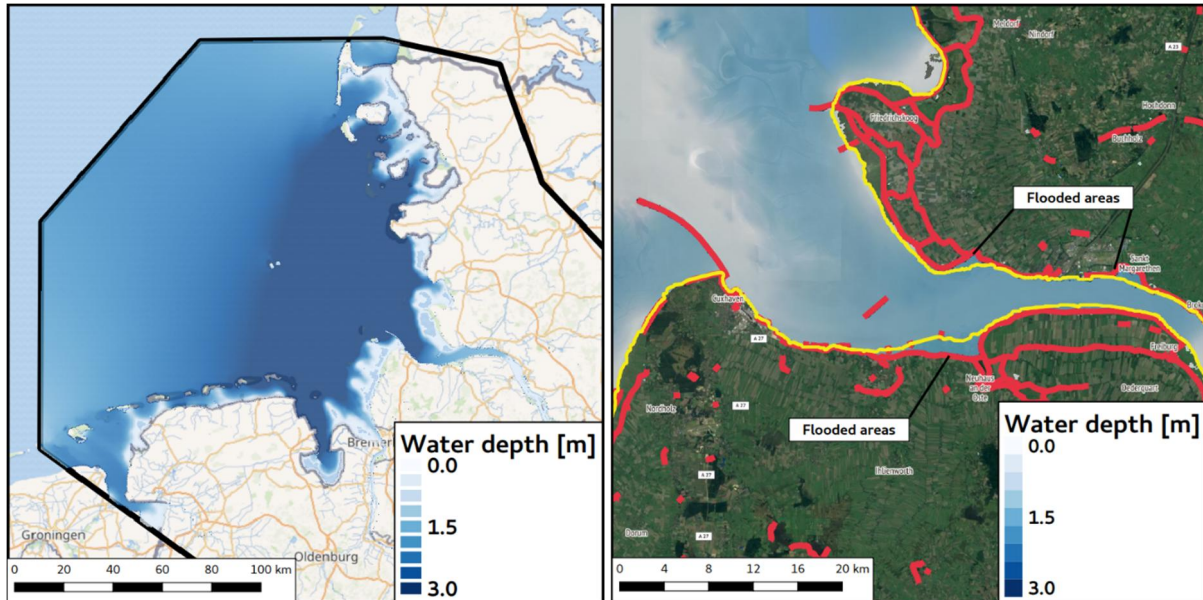


Figure 15. Storm Xaver, as simulated by ANUGA when the storm surge hits the coast of Germany. On the left, the overview of the case study area as the storm hits the coastline. On the right, a highlight of flooded areas close to the city of Cuxhaven (the presence of dykes are shown in red; the coastline is shown in yellow, water depth is shown in shades of blue).

4.2.2 Asset damage to critical infrastructure

Infrastructure damages due to storm Xaver are widespread along the coastline of Northern Germany, resulting in a total asset damage of approximately 13 million euros. Figure 16 shows the spatial distribution of damaged infrastructure; whereby further detail of the aggregated damages is given to Hamburg.

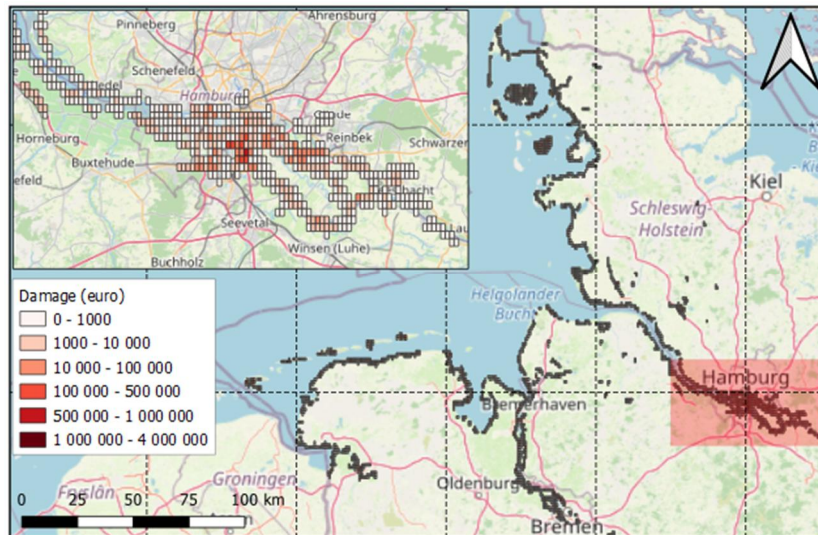


Figure 16. The spatial distribution of locations that suffer damages to critical infrastructure along the coastline of Northern Germany due to storm Xaver, with a detailed overview of the aggregated damages for Hamburg.

The damages categorized per CI system (see table 1 for classification) are presented in Figure 17. It shows that the highest damage is to the CI system transportation (32.1%), followed by education (30.5%), and waste (30.0%). The remaining 7.3% of the total damage is a result of damaged assets within the healthcare, water, and energy CI system. Although multiple telecommunication assets are exposed to flooding induced by storm Xaver, they are not damaged.

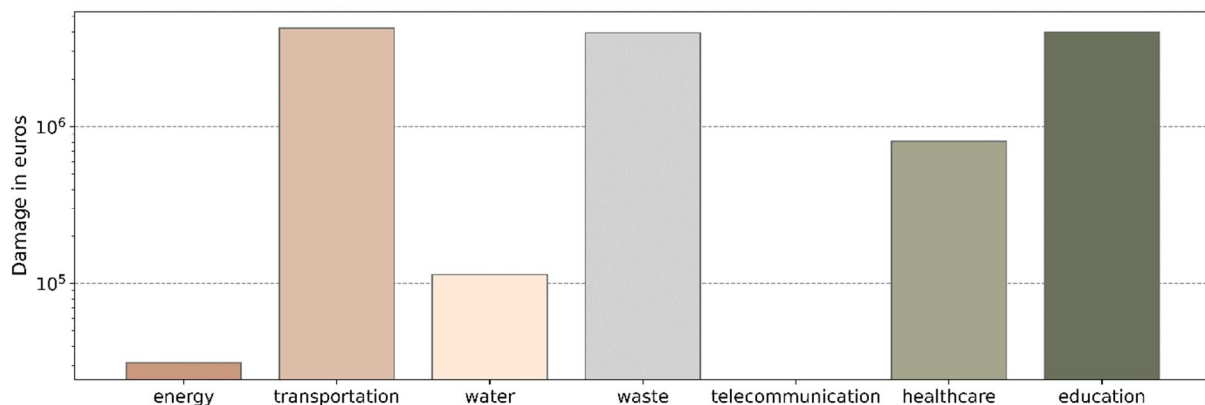


Figure 17. Damages (in euros) to critical infrastructure categorized per overarching CI system due to storm Xaver

The relative contribution of the damage per infrastructure type with a further specification per CI system are displayed in Figure 18. Every infrastructure type within the hardest-hit CI system transportation experiences damage due to flooding. Again, the road network has the highest contribution to the total damage within the CI system; flooding results in 2.4 million euro in road damages. Exposed railways translate into 1.6 million euro in damages. Wastewater treatment plants predominantly contribute with 99% to the overall damage of the second-hardest hit CI

system 'waste', with waste transfer stations contributing to the remainder of damages (figure 18). The island Juist is one of the seven East Frisian islands that suffers from flooding, most notably resulting to high damages to an inundated wastewater treatment plant.

A total of 42 education facilities are exposed to flooding, with schools being the most severely affected (3.2 million euro), followed by kindergartens, universities and colleges (Figure 18). When considering the health CI system, four types of health facilities are compromised due to coastal flooding: clinic (41%), rehabilitation (31%), hospital (24%) and doctors (3%). Furthermore, the total damage to the energy system is relatively low, with most of the damages occurring to power plants (figure 18). Generally, these exposed plants, however, experience low levels of inundation, thereby limiting the damage.

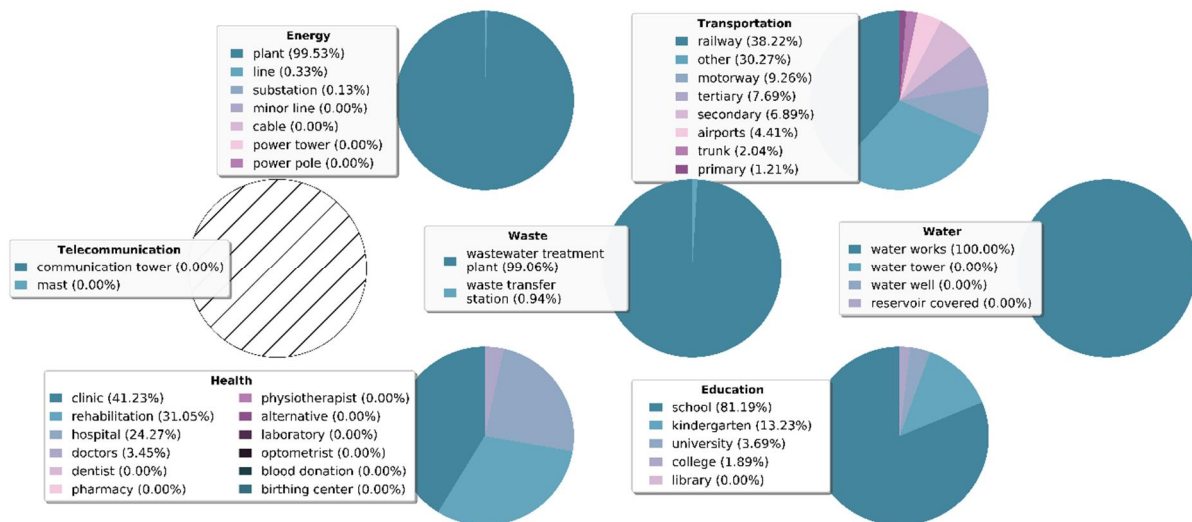


Figure 18. Relative asset damages per infrastructure type for each overarching CI system due to storm Xaver

4.2.3 Wider economic impacts of infrastructure failure

For storm Xaver, we have estimated economic losses to be approximately 2.1 million Euro a day for the entire European Union as a result of infrastructure failure due to flooding (see section 3.3.3) in the northwestern part of Germany. If we would only focus on the economic impacts to the affected region considered in this analysis for storm Xaver, the model results show a daily impact of approximately 7.4 million Euro a day. In the whole of Germany, the daily losses amount to approximately 3.2 million Euro a day. Figure 19 presents the relative impacts per sector in absolute and relative terms for the affected region only, the country and the wider economic impacts to the entire European Union.

In relative terms, most services sectors are affected similarly, which is a direct artifact of how the impacts are modelled (a production disruption due to flooded infrastructure). Due to the relatively small amount of industry affected (around 2.5%), the cascading effects within the region and beyond are limited. Interestingly, in relative terms, the highest affected sector is the mining and quarrying sector. Similar to the consequences of infrastructure failure for storm Xynthia (Section 4.1.3), this sector is again only affected indirectly through supply chain disruptions. Manufacturing again shows clear substitution effects when increasing the spatial scale, whereas wholesale and retail show a small increase in impacts when moving from country to European impacts. This could be explained by the fact that one of affected areas is Bremerhaven, which will have direct trade links to regions outside Germany as well.

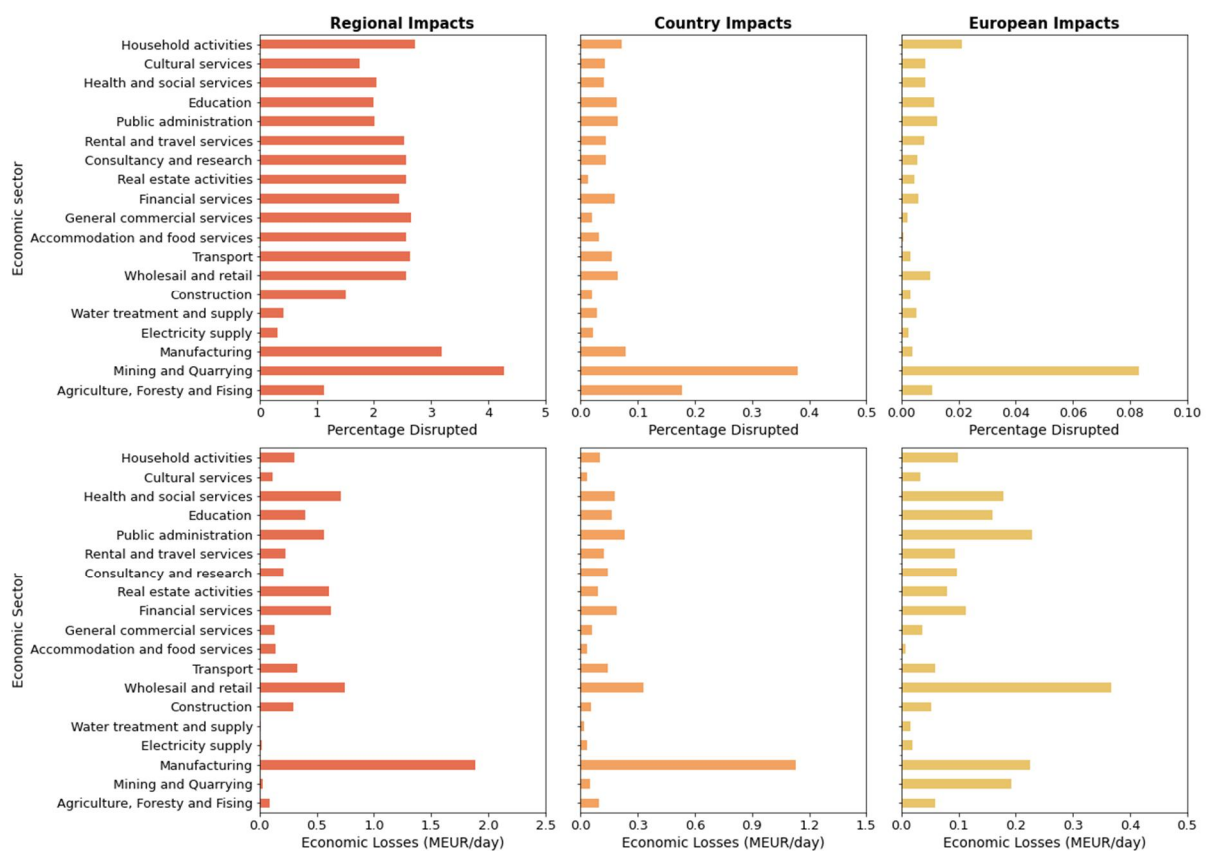


Figure 19. Daily economic impacts on a Regional (directly affected regions), country (directly affected country) and European level as a result of infrastructure failure due to storm Xaver.

4.3 November 2002 Storm Surge in Emilia-Romagna

4.3.1 Extreme sea-level and coastal inundation

Sea level at the Italian coast along the Emilia-Romagna Region reached record highs during a series of storm surge events in November 2002 (see Figure below), the highest of which was recorded between the 15th and 16th of November 2011. The peak was the result of a

combination of high surge, high tide and wave height coinciding in time. The maximum wave height of 4.8 m has been registered at the Ancona-Mar1 station, while wave direction was mostly at 116° north, thus in direction of the coastline of the Emilia-Romagna Region (ISPRA, 2005; Perini et al., 2011).

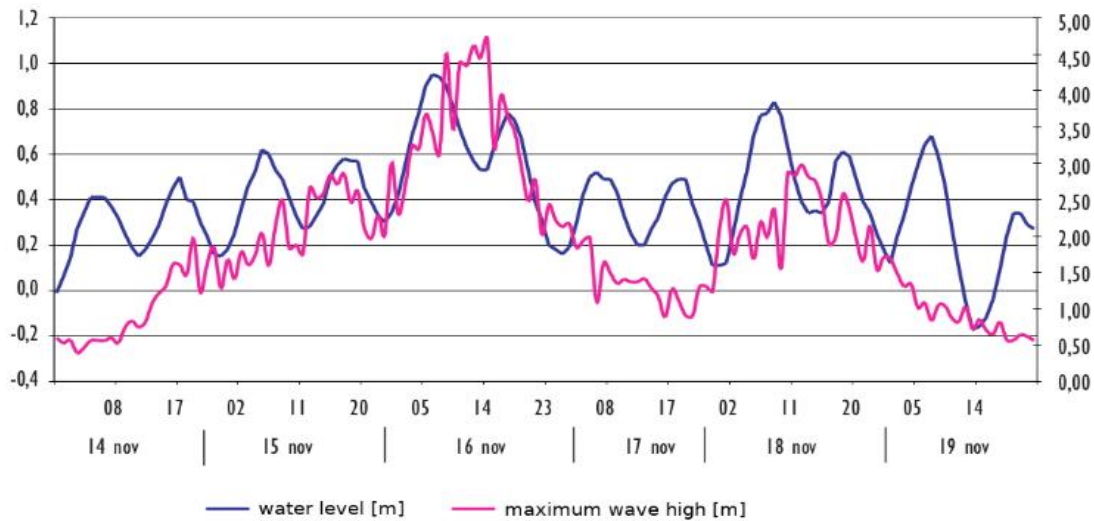


Figure 20 Observed sea level and wave height along the Emilia-Romagna coast (Ancona-Mar1 station) in Italy during the November 2002 events. The left y-axis indicates the mean water level. The right y-axis indicates the maximum wave height. Adapted from Perini et al., 2011.

The coastal inundation process was simulated using the ANUGA model. Extreme water levels and wave dynamics are incorporated in ANUGA by considering the information available in historical datasets (ISPRA, 2005; Perini et al., 2011). The inundation process is simulated at the maximum water level height of the event, thus starting on the 15th and finishing on the 16th November 2002. For the case of the Emilia-Romagna Coast, we include the influences of waves by simulating a series of waves hitting the coast of Emilia-Romagna with a wave period of 7.1 seconds (ISPRA, 2005). We incorporate the presence and height of coastal flood defences by relying on LiDAR data available along the coastal zone of Italy¹. Figure 21 displays the water level distribution along the coastline of the Emilia-Romagna Region during the maximum simulated water levels. As observed, coastal flooding is observed near the cities of Rimini, Cesenatico, and Cervia.

¹ <http://www.pcn.minambiente.it/mattm/en/pst-project-lidar-data/>



Figure 21. The storm surge event of 15 November 2002, as simulated by ANUGA when the storm surge hits the city of Rimini. In red, the area where the coastal defense project called "Parco del Mare" is located. The yellow line indicates the coastline. Flooded areas are indicated in shades of blue, according to the water depth.

4.3.2 Asset damage to critical infrastructure

Coastal flooding in the Emilia-Romagna Region results in damaged infrastructure along the entire length of the coast. Particularly in the coastal towns Ravenna, Cervia, Cesenatico and Rimini total asset damages can reach up to millions of euros. Figure 22 shows the spatial distribution of damaged infrastructure, whereby further detail of the aggregated damages is given to Rimini, Cesenatico and surroundings.

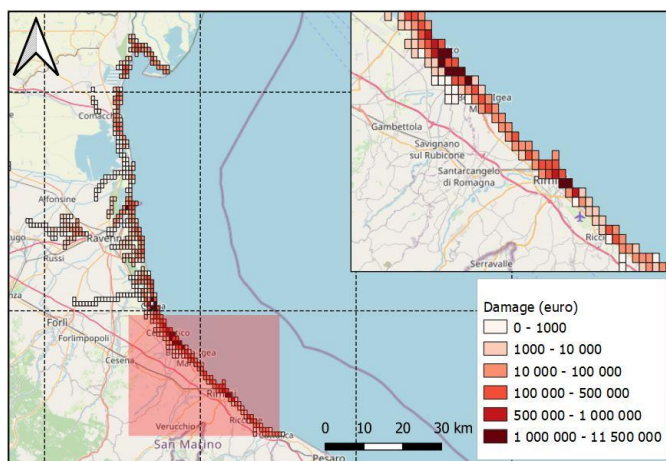


Figure 22. The spatial distribution of locations that suffer damages to critical infrastructure along the coastline of the Emilia-Romagna Region due to flooding, with a detailed overview of the aggregated damages for Rimini and surroundings

Critical infrastructure situated along the coast in the Emilia-Romagna region exposed to the flooding resulted in a total damage of 80.1 million euros. The damage to the education facilities amounts 32.7 million euros and has therefore the highest contribution (40.5%) to the overall damage to critical infrastructure. The transportation system also suffers a considerably high damage, namely 24.8 million euros (31.1% of the total damage). This is then followed by the CI system healthcare (14.8%), energy (13.7%), and telecommunication (0.3%).

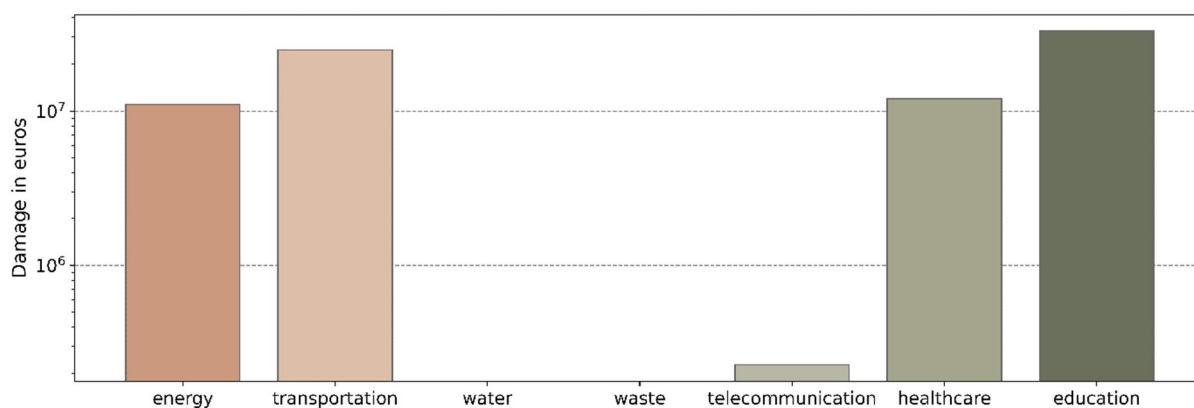


Figure 23. Damages (in euros) to critical infrastructure categorized per overarching CI system due to flooding in Emilia-Romagna

The relative damages per infrastructure type specified per CI system are represented in Figure 24. We find that 85 education and health facilities are located in flood-prone areas, which translates into particularly high damages to schools (30 million euros) and hospitals (8 million euros). The road network accounts for 85% of the total damages within the transportation system, while the remainder is due damages to multiple parts of the railway network and one small-scale aerodrome in Ravenna. The damages within the energy system are predominantly caused by flooded a plant in the industrial area of Ravenna and a substation in Cervia, resulting in 9.6 and 1.3 million euro in damage, respectively.

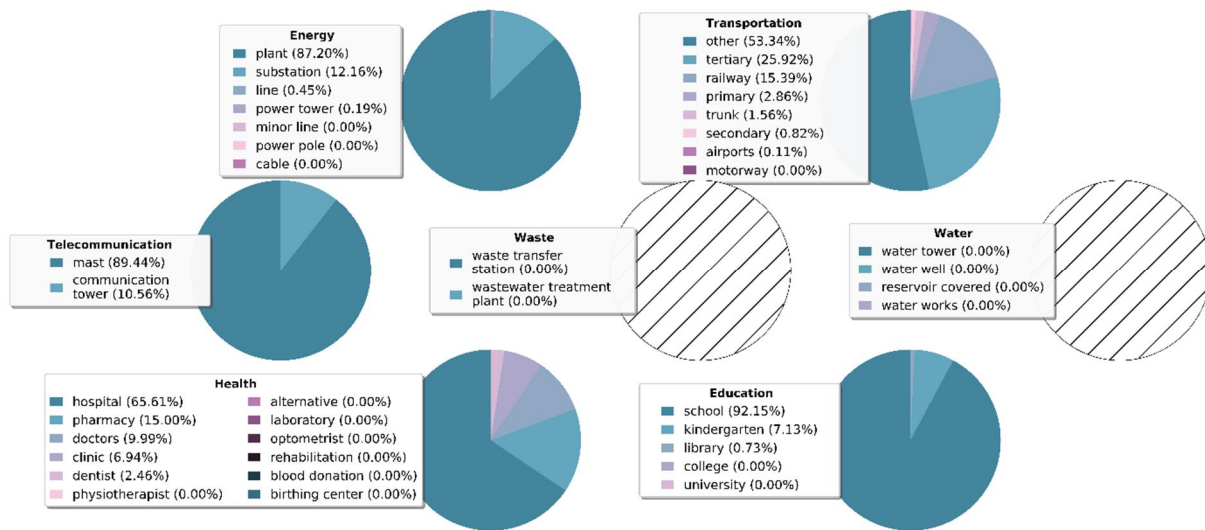


Figure 24. Relative asset damages per infrastructure type for each overarching CI system due to flooding in Emilia-Romagna

4.3.3 Wider economic impacts of infrastructure failure

For the flood event in Emilia Romagna, we have estimated an economic impact of approximately 0.9 million Euro a day for the entire European Union as a result of infrastructure failure due to coastal flooding in Emilia Romagna. If we would only focus on the economic impacts to Emilia Romagna, the model results show a daily impact of approximately 7.4 million Euro a day. For the entire Italy, the daily losses amount to approximately 1.7 million Euro a day. Figure 25 presents the relative impacts per sector in absolute and relative terms for the Emilia Romagna only (left-most panels), Italy (middle panels) and the wider economic impacts to the entire European Union (right-most panels).

The results show again similar results for the mining and quarrying sector, indicating that this sector is particularly vulnerable to supply chain disruptions. Similarly, manufacturing and wholesale and retail are in absolute terms again one of the most affected sectors. Interestingly, compared to Xaver for which the daily impacts are roughly the same for the affected region, we find overall much smaller impacts on a country and European level. This could be explained by the fact that Xaver affected the port of Bremerhaven, which has much more linkages with other regions compared to the region of Emilia Romagna.

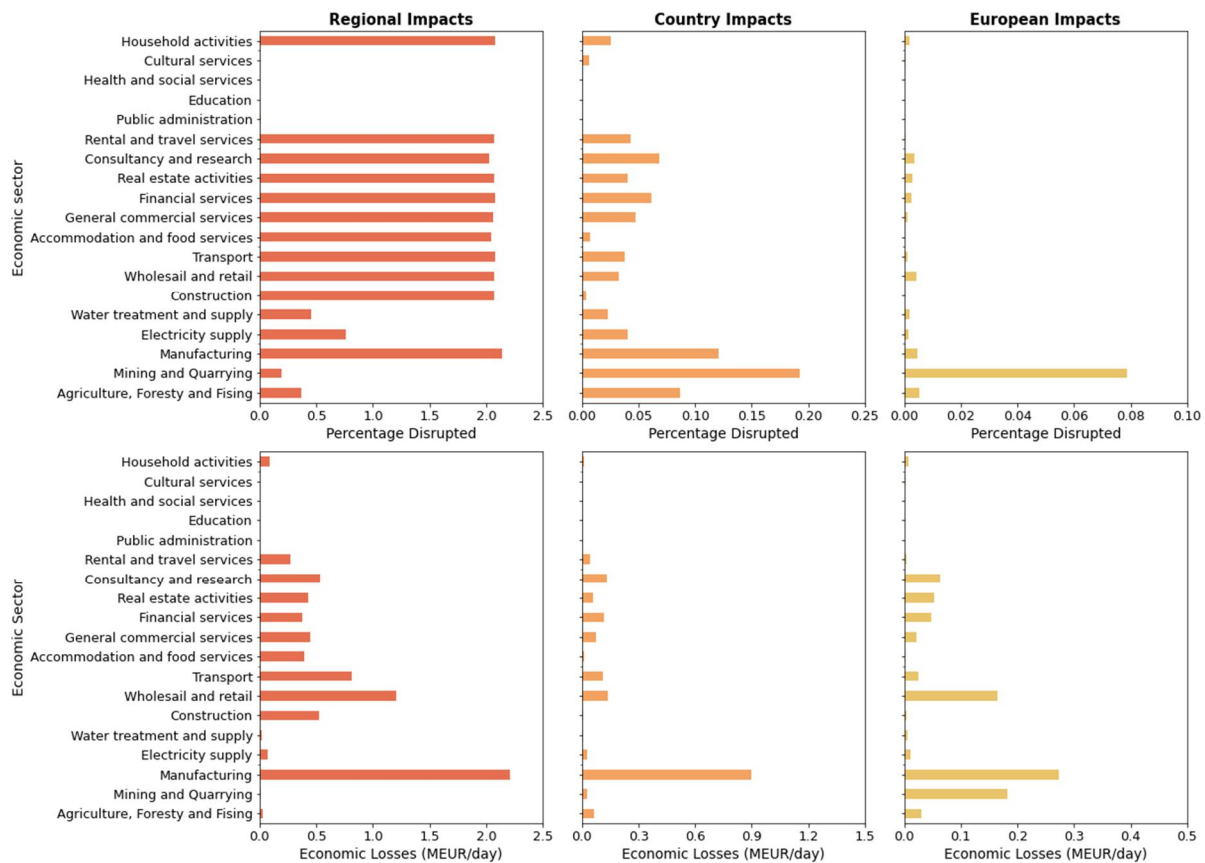


Figure 25. Daily economic impacts on a Regional (directly affected regions), country (directly affected country) and European level as a result of infrastructure failure due to the November 2002 Storm Surge in Emilia-Romagna.

5 Discussion

Storm Xynthia led to flooding along the Atlantic coast of France. Due to high exposure to storm surge events, most of the Atlantic coast of France is protected by the presence of coastal defence structures, some of which are natural. During the Storm Xynthia event, coastal flooding was observed mostly around the cities of La Faute-sur-Mer, L'Aiguillon-sur-Mer, and La Rochelle. The collapse of the seawall near the city of L'Aiguillon-sur-Mer played a major role in the flooding process around that area (see Figure 9). Significant agricultural lands and open fields in the Bay of l'Aiguillon are also simulated as flooded.

With regards to Storm Xaver, minimal flooding was observed along the coast of Germany (see Figure 15). The North Sea coast of Germany is subject to significant variations of tide level, where tidal range varies between about 1 to 4 meters. Historically, the area is frequently exposed to storm surge events. As a result, the coastline of Germany's North Sea is mostly defended by the presence of man-made coastal defenses. The primary impact to the energy sector were large scale electrical power loss and damaged wind turbines in parts of Germany. Coastal flooding was reported in Hamburg and in few other locations along the German

coastline. The simulation of the event with ANUGA indicates minimal flooding along the German North Sea coast, mostly due to the consideration of coastal defense structures into the flood modelling.

With regards to the Emilia-Romagna Region coastal flooding event of November 2002, coastal flooding is simulated near the cities of Rimini (see Figure 21), Cesenatico, and Cervia. Indeed, this was the case in reality, where flooding was reported along the Riminese coastline. In this context, the municipality of Rimini is currently implementing an urban renovation project to promote citizens welfare while increasing the protection to extreme sea levels, called "Parco del Mare". A similar solution is also currently under consideration in the municipality of Cesenatico. Such adaptation measures could be taken into account in our modelling chain by merging the barrier into the existing bed elevations.

For the risk modelling of the asset damages, we have collected vulnerability data, both the fragility curves and the associated maximum damages, from the current body of literature. We encountered multiple challenges associated with vulnerability data for CI. Firstly, the current body of literature provides limited information on vulnerability of CI. For example, energy and transportation are CI systems that are generally well-covered, but CI systems as waste and telecommunication are less covered or not covered at all. Assumptions needed to be made for infrastructure types that lacked fragility curves and/or maximum damages. For example, no vulnerability curves exist for waste transfer stations. Here, we assumed that vulnerability data used for industry can be used for the solid waste infrastructure. Secondly, even if vulnerability data is available, it is not always clear in what way they are derived and how they can be applied. For example, Kok et al. (2005) provides a maximum damage value of 1197 euro/m² for airports, but it is unclear how this value is derived (e.g., what components of an airport are included?). We believe that the usage of this maximum damage leads to an overestimation of the airport damages, and therefore adapted an approach to identify components in airports (i.e., runways and terminals) that may be at risk.

6 Concluding remarks and next steps

The methodology as described in this report can be seen as the starting point for the assessment of future storylines. We provide here a front-to-end methodology, that starts with the estimation of extreme sea-levels as a result of three specific storms (Xynthia, Xaver and 2002 Emilia Romagna storm surge event), followed by an inundation modelling exercise to estimate inundation levels along the coastline. Using these inundation maps, we can estimate the direct asset damage to critical infrastructure along the coast and the indirect economic impacts as a result of the failure of this infrastructure.

The results show estimated direct damages to critical infrastructure of 11.3 million Euro, 13 million Euro and 80 million Euro, for respectively Xynthia, Xaver and the storm surge event in Emilia Romagna. The wider economic losses are estimated to be around 24 million Euro a day for the affected regions of storm Xynthia (7 million Euro a day for the whole of Europe due to substitution effects). For storm Xaver, the estimated daily economic impacts are approximately 7 million Euro a day for the affected regions in Northern Germany, with around 2 million Euro a day for the whole of Europe. For the storm surge event in Emilia Romagna, the local impacts are approximately 7.4 million Euro a day, with approximately 0.9 million Euro a day for the entire Europe. The results show a clear decrease in the absolute impacts with larger spatial scales. This indicates a clear substitution effect. While substitution is limited within the affected region (everyone is in some way affected, making it hard to take over some production), it is possible for non-affected regions to take over some of the demand and supply that is not satisfied anymore by the affected region.

While not included yet in this analysis, for the future situation, one should account for changes in all components of risk (e.g., hazard, exposure and vulnerability). Changes in the hazard, represented through extreme sea-level rise and coastal flooding, will be modelled under different future warming levels. These future warming levels will drive, amongst others, melting of the west Antarctic ice-sheet, which will influence extreme sea levels in Europe during (extra)tropical storms.

Changes in exposure will be modelled through finding relations between infrastructure density (represented by the CISI-index), GDP and population for the present situation. Using these relations, we can use spatially explicit GDP and population future projections that are built upon the Socioeconomic Shared Pathways (SSP) to estimate future infrastructure density. We cannot assume, however, that countries simply expand their infrastructure inventory without considering adaptation, in particular under higher warming levels where the threat of coastal flooding increases. As such, for storylines describing the future situation, we will consider different adaptation strategies (both regional and asset-level) to assess how adaptation will alter the potential impact of coastal flooding in Europe.

7 Bibliography

- Bertin, Xavier, Nicolas Bruneau, Jean-François Breilh, André B. Fortunato, and Mikhail Karpytchev. "Importance of Wave Age and Resonance in Storm Surges: The Case Xynthia, Bay of Biscay." *Ocean Modelling* 42 (January 1, 2012): 16–30. <https://doi.org/10.1016/j.ocemod.2011.11.001>.
- Burns & McDonnell (n.d.). Impacts on underground transmission assets due to flooding caused by major storms. Power Delivery Intelligence Initiative (PDI2).
- Carruthers, R., 2013. What prospects for transport infrastructure and impacts on growth in southern and eastern Mediterranean countries?
- Charnock, H. "Wind stress on a water surface." *Quarterly Journal of the Royal Meteorological Society* 81, no. 350 (1955): 639–40. <https://doi.org/10.1002/qj.49708135027>.
- Chauveau, E., Chadenas, C., Comentale, B., Pottier, P., Blanloeil, A., Feuillet, T., Mercier, D., Pourinet, L., Rollo, N., Tillier, I. & Trouillet, B. (2017). Xynthia: lessons learned from a catastrophe. *Cybergeo. European Journal of Geography*. <https://doi.org/10.4000/cybergeo.28032>.
- CPSL (2005). Coastal Protection and Sea Level Rise - Solutions for sustainable coastal protection in the Wadden Sea region. Wadden Sea Ecosystem No. 21. Common Wadden Sea Secretariat, Trilateral Working Group on Coastal Protection and Sea Level Rise (CPSL), Wilhelmshaven, Germany.
- Dangendorf, Sönke, Arne Arns, Joaquim G Pinto, Patrick Ludwig, and Jürgen Jensen. "The Exceptional Influence of Storm 'Xaver' on Design Water Levels in the German Bight." *Environmental Research Letters* 11, no. 5 (May 1, 2016): 054001. <https://doi.org/10.1088/1748-9326/11/5/054001>.
- Deuschländer, T., Friedrich, K., Haeseler, S. & Lefebvre, C. (2013). Severe storm XAVER across northern Europe from 5 to 7 December 2013. Deutscher Wetterdienst.
- EEA (2020) Corine Land Cover 2018. Copernicus Land Monitoring Service, European Environmental Agency. Copenhagen, Denmark.
- FEMA (2013). Hazus-MH2.1, Multihazard Loss Estimation Methodology, Flood Model Technical Manual. Federal Emergency Management Agency, Washington DC, USA.
- Foster, N.G. (2015). "How much does a cell tower cost?" Retrieved from <https://www.airwaveadvisors.com/blog/how-much-does-a-cell-tower-cost/>
- Gibson, G., Milnes, R., Morris, M., Hill, N., Simbolotti, G., Tosato, G., 2011. Aviation Infrastructure, Energy Technology Systems Analysis Programme.
- Hall, K.L. (2009). An updated study on the undergrounding of overhead power lines. Edison Electric Institute, Washington DC, USA.
- Horsburgh, K., Haigh, I. D., Williams, J., De Dominicis, M., Wolf, J., Inayatillah, A., & Byrne, D. (2021). "Grey swan" storm surges pose a greater coastal flood hazard than climate change. *Ocean Dynamics*, 1-16.
- Huizinga, J., de Moel, H. & Szewczyk, W. (2017). "Global flood depth-damage functions: Methodology and database with guidelines." Publications Office of the European Union, Luxembourg, Luxembourg. <https://doi.org/10.2760/16510>, 110 pp., 2017.
- ISPRA (2005). Sezione B: Eventi di mareggiata (Onde Alte e Mareggiate) per settori e tratti costieri pag. 2. Settore costiero C1: Portofino – C.po Linaro pag. 3. Available at: <https://www.isprambiente.gov.it/files/atlan-te-coste/eventi-di-mareggiata1.pdf>
- Kellermann, P., Schöbel, A., Kundela, G. & Thieken, A. H. (2015). "Estimating flood damage to railway infrastructure – the case study of the March River flood in 2006 at the Austrian

- Northern Railway." *Nat. Hazards Earth Syst. Sci.*, 15, 2485–2496, <https://doi.org/10.5194/nhess-15-2485-2015>, .
- Kernkamp, Herman W. J., Arthur Van Dam, Guus S. Stelling, and Erik D. de Goede. "Efficient Scheme for the Shallow Water Equations on Unstructured Grids with Application to the Continental Shelf." *Ocean Dynamics* 61, no. 8 (August 1, 2011): 1175–88. <https://doi.org/10.1007/s10236-011-0423-6>.
- Kettle, A.J. (2020). "Storm Xaver over Europe in December 2013: Overview of energy impacts and North Sea events." *Advances in Geosciences* 54: 137-147. <https://doi.org/10.5194/adgeo-54-137-2020>
- Kok, M., Huizinga, H.J., Vrouwenfelder, A.C.W.M. & Barendregt (2005). Standard method 2004 Damage and Casualties by flooding. Ministerie van Verkeer en Waterstaat, Rijkswaterstaat, Nederland.
- Kolen, B., Slomp, R., van Balen, W., Terpstra, T., Bottema, M. & Nieuwenhuis, S. (2010). Learning from French experiences with storm Xynthia: Damages after a flood. HKV and Rijkswaterstaat.
- Kolen, B., Slomp, R. & Jonkman, S.N. (2013). "The impacts of storm Xynthia February 27-28, 2010 in France: lessons for flood risk management". *Journal of Flood Risk Management* 6, no. 3: DOI: 10.1111/jfr3.12011
- Liebman, D.J. (2018). "Cell tower leases add big value with little maintenance." Retrieved from <https://blog.sior.com/cell-tower-leases-add-big-value-with-little-maintenance#:~:text=The%20average%20cost%20to%20build,leases%20for%20some%20property%20owners>
- MISO (2021). Transmission cost estimation guide: for MTEP21.
- Miyamoto (2019). Overview of Engineering Options for Increasing Infrastructure Resilience. Washington, D.C., World Bank Group.
- Muis, S., Verlaan, M., Winsemius, H. C., Aerts, J. C., & Ward, P. J. (2016). A global reanalysis of storm surges and extreme sea levels. *Nature communications*, 7(1), 1-12.
- Perini L., Calabrese L., Deserti M., Valentini A., Ciavola P., Armaroli C., (2011). Le mareggiate e gli impatti sulla costa in Emilia-Romagna 1946-2010. Arpa Emilia-Romagna. ISBN: 88-87854-27-5
- Risk Management Solutions (2014). 2013-2014 winter storms in Europe: an insurance and catastrophe modeling perspective.
- Rucińska, D. (2019). "Describing Storm Xaver in disaster terms." *International Journal of Disaster Risk Reduction* 34: 147-153. <https://doi.org/10.1016/j.ijdr.2018.11.012>
- Shepherd, T. G., Boyd, E., Calel, R. A., Chapman, S. C., Dessai, S., Dima-West, I. M., ... & Zenghelis, D. A. (2018). Storylines: an alternative approach to representing uncertainty in physical aspects of climate change. *Climatic change*, 151(3), 555-571.
- Sillmann, J., Shepherd, T. G., van den Hurk, B., Hazeleger, W., Martius, O., Slingo, J., & Zscheischler, J. (2021). Event-Based Storylines to Address Climate Risk. *Earth's Future*, 9(2), e2020EF001783.
- Spencer, T., Brooks, S.M., Evans, B.R., Tempest, J.A. & Möller, I. (2015). "Southern North Sea storm surge event of 5 december 2013: water levels, waves and coastal impacts." *Earth-Science Reviews* 146: 120-145. <https://doi.org/10.1016/j.earscirev.2015.04.002>
- van Ginkel, K. C. H., Dottori, F., Alfieri, L., Feyen, L., and Koks, E. E. (2021). "Flood risk assessment of the European road network." *Nat. Hazards Earth Syst. Sci.*, 21, 1011–1027, <https://doi.org/10.5194/nhess-21-1011-2021>.

Wadey, M.P., Haigh, I.D., Nicholls, R.J., Brown, J.M., Horsburgh, K., Carroll, B., Gallop, S.L., Mason, T. & Bradshaw, E. (2015). "A comparison of the 31 January–1 February 1953 and 5–6 December 2013 coastal flood events around the UK." *Frontiers in Marine Science* 2, no. 84. doi: 10.3389/fmars.2015.00084



Receipt

